Wetting and Minimal Surfaces

Constantin Bachas[1,2], **Pierre Le Doussal**[1], **Kay Jörg Wiese**[1]

[1] *CNRS-Laboratoire de Physique Théorique de l'Ecole Normale Supérieure, 24 rue Lhomond, 75231 Cedex 05, Paris, France.*

[2] *Institut für Theoretische Physik, ETH Zürich, 8093 Zürich, Switzerland.*

(Dated: June 26, 2006)

We study minimal surfaces which arise in wetting and capillarity phenomena. Using conformal coordinates, we reduce the problem to a set of coupled boundary equations for the contact line of the fluid surface, and then derive simple diagrammatic rules to calculate the non-linear corrections to the Joanny-de Gennes energy. We argue that perturbation theory is quasi-local, i.e. that all geometric length scales of the fluid container decouple from the short-wavelength deformations of the contact line. This is illustrated by a calculation of the linearized interaction between contact lines on two opposite parallel walls. We present a simple algorithm to compute the minimal surface and its energy based on these ideas. We also point out the intriguing singularities that arise in the Legendre transformation from the pure Dirichlet to the mixed Dirichlet-Neumann problem.

I. INTRODUCTION

Minimal surfaces, i.e. surfaces of minimal area with specified boundary conditions, are found in many areas of physics, mathematics and biology. Their existence, uniqueness and other properties (such as possible singularities or stability) are still actively studied by mathematicians [1]. In the laboratory, minimal surfaces are most commonly realized as soap films bounded by a given wire-frame, a problem discussed already in 1873 by Plateau [2]. In some cases their morphology and stability have actually been elucidated experimentally in this context [3]. Other systems where minimal surfaces play a role include lipid-water solutions, diblock copolymers, crystallography, protein structure, or liquid crystals such as smectics [4]. They also arise as world-sheet instantons in string theory, for example in the semiclassical, fixed-angle high-energy limit of scattering amplitudes [5].

The minimal surfaces that will interest us here arise in the problem of partial wetting of a solid by a liquid [6]. In the standard experimental situation, a liquid with free surface of area $\mathcal{A}$ (liquid-air interface) wets a flat solid plane over an area $\mathcal{A}'$ (liquid-solid interface). The free surface meets the solid plane along a line, called *contact line*, at an angle θ which is defined locally. The interfacial energy is the difference $\mathcal{E} = \gamma\mathcal{A} - \gamma'\mathcal{A}'$, where γ is the energy per unit area (or surface tension) of the liquid-air interface, and $\gamma' = \gamma_{SA} - \gamma_{SL}$ is the difference in surface tension between the solid-air (SA) and the solid-liquid (SL) interfaces. The force per unit length pushing a segment of the contact line towards the unwetted region is thus $f = -\gamma\cos\theta + \gamma'$. Requiring that it vanishes gives Young's [7, 8] local equilibrium condition, $\theta = \arccos(\gamma'/\gamma)$. The minimal-surface problem at hand is thus a problem with *mixed Neumann and Dirichlet* boundary conditions. In the idealized setting of an infinite liquid container and a perfectly homogeneous planar wall, there exists a simple solution to this problem: it is a planar liquid-air interface meeting the wall along a straight contact line. Strictly-speaking, as we will discuss in section II, the properties of the container at infinity must be carefully chosen in order not to destabilize this solution.

Two extra forces play in fact a role in the general formulation of the wetting problem. The first comes from the drop in pressure across the liquid-air interface, which adds to the Gibbs energy a volume term: $\mathcal{E} = \gamma\mathcal{A} - \gamma'\mathcal{A}' - pV$. Here p is the pressure difference and V the volume of the fluid. The free surfaces that minimize this energy have constant rather than vanishing mean curvature [8]. It is quite remarkable that the corresponding equations are (at least formally) integrable, see for instance [9]. Note that in the special case of an incompressible fluid, p is a Lagrange multiplier determined by the constraint that the "droplet" volume V be fixed. The second force that plays in general a role is gravity, which introduces an additional scale, the capillary length $\kappa^{-1} = (\gamma/\rho g)^{1/2}$. Here ρ is the fluid mass density, and g is the gravitational acceleration. In this paper we will study situations where both pressure and gravity can be ignored. This is usually valid if one concentrates on length scales $\ll \kappa^{-1}$, and considers a fluid connected to an infinite reservoir so that effectively $p \simeq 0$. Note that the capillary length is typically of the order of a few millimeters, but it can be made much larger in free-fall (e.g. space-based) experiments, or if one replaces the air by a second non-mixing fluid of roughly equal mass density. Thus setting $\kappa \simeq p \simeq 0$ is a good approximation in a wide range of experimentally-feasible situations, and we will do so in this paper. Technically, one can further justify that gravity be ignored *at all scales* if a condition, identified below, is satisfied.

What is in fact more questionable is the assumption of a perfectly homogeneous wall. Indeed, in most of the experimental setups of wetting, roughness and impurities of the solid substrate couple directly to the position of the contact line, which may as a result be effectively pinned. Computing the energy of a *deformed* contact line is thus a question of foremost importance. For small deformations, as Joanny and de Gennes (JdG) have shown [10], the contact line obeys *non-local linear elasticity*. These linear equations may become unstable at wavelengths comparable to some global-geometry scale, as several earlier studies have established [11]. The issue of non-linear elasticity, which becomes relevant for larger deformations, has been addressed only

recently [12]. It could play a role [13] in resolving the apparent disagreement between recent experimental measurements of contact-line roughness [14], and renormalization-group calculations near the depinning transition [15] or numerical simulations [16] that were based on the JdG linear theory [17]. To be sure, hysteresis and other dynamical phenomena, which have attracted much of the recent attention [18], may also prove important in interpreting the above experimental data. Nevertheless, a systematic analysis should start with a thorough understanding of the non-linear and possibly non-local effects in the simpler, equilibrium situation. This is the problem that we will study here.

The area of a minimal surface bounded by a given (closed) curve is simple when expressed in conformal coordinates. Non-linearities arise because this choice of coordinates depends non-trivially on the boundary curve, through the conformal-gauge (or Virasoro) conditions. In this paper we develop systematic methods for solving the ensuing non-local and non-linear equations, either in perturbation theory or numerically. We focus, in particular, on the case of a planar wall, and derive simple diagrammatic rules that calculate the energy of a deformed contact line to any given order in the deformation amplitude. The method can be extended to more complicated container geometries, but the details become more involved. As a relatively simple illustration, we show how to extend the rules, and calculate the JdG linear theory, in the case of two contact lines lying on parallel opposite walls. We also describe a novel algorithm which finds the minimal surface energy with no need for surface triangulation. Finally, we discuss some general properties of these perturbative expansions, which bear a fascinating similarity to problems encountered in perturbative string theory. We hope to return to some of these questions, as well as to the implications of our results for the wetting problem, in a future publication.

The paper is organized as follows: In section II we describe our basic model, point out the need for global tadpole cancellation, and discuss the relation of the mixed Neumann/Dirichlet to the pure Dirichlet problem. In section III we give the formal solution of the latter problem, for an arbitrary boundary curve, in terms of conformal coordinates. This is standard material which is included here for completeness. In section IV we specialize to the case of a planar wall, derive the corresponding non-linear boundary equations, and express the energy in terms of their solution. We pay particular attention to the decoupling of the large-volume cutoff, which as we will explain is rather subtle. In section V we solve the boundary equations perturbatively, and compute the corrections to the JdG energy, up to quartic order. Section VI describes an alternative approach, using Lagrange-multiplier fields and leading to a simple diagrammatic representation of the perturbative expansion. The numerical algorithm is presented in Section VII. In section VIII we extend this to the case of two parallel walls, and calculate the quadratic interaction of the contact lines. Finally, in section IX we establish the finiteness of the perturbative expansion order by order, and point out some intriguing directions for future work. The Weierstrass parameterization of our fluid surfaces, a calculation confirming the decoupling of the large-volume cutoff are described, respectively, in appendices A and B.

II. THE MODEL

We consider a fluid inside a tubular container $\Omega \times \mathbb{R}$, where $\mathbb{R}$ corresponds to the height coordinate z, and Ω is some (a priori arbitrary) connected region in the (x, y) plane, with boundary $\partial\Omega$. Let us for now assume that the fluid surface has no overhangs – it can then be parameterized by the height function $z(x, y)$. We may express the energy functional as the following sum of two-dimensional bulk and boundary terms:

$$\mathcal{E} = \mathcal{E}_{\rm bulk} + \mathcal{E}_{\rm bnry} = \int_\Omega {\rm d}x\,{\rm d}y\,\left(\gamma\sqrt{1+(\partial_x z)^2\,+\,(\partial_y z)^2}\;-\;pz+\frac{1}{2}\rho g z^2\right) - \int_{\partial\Omega}{\rm d}l\,\gamma'(l)\,z\;\;, \tag{1}$$

where ${\rm d}l$ is the infinitesimal length along the boundary of Ω. The first term in (1) is the fluid-air interfacial energy $\gamma\mathcal{A}$, the second is due to the difference in pressure between air and fluid, the third to gravity, while the last comes from the fluid-solid interface. For convenience, we have slightly generalized the model so that the tension of this interface may vary along the container walls, as can be done by design. The more general case of a γ' depending on both l and z, due for instance to the presence of impurities, will be discussed below. For now γ' is only a function of l.

In the absence of gravity $g = 0$, the minimum of the energy $\mathcal{E}$ is a surface of constant mean curvature, with specified contact angles:

$$\vec\nabla\cdot\left(\frac{\vec\nabla z}{\sqrt{1+|\vec\nabla z|^2}}\right) = -\frac{p}{\gamma} \qquad \text{and} \qquad \left.\frac{\widehat{n}\cdot\vec\nabla z}{\sqrt{1+|\vec\nabla z|^2}}\right|_{\partial\Omega} = \cos\theta(l) \;=\; \frac{\gamma'(l)}{\gamma}\,, \tag{2}$$

where $\vec\nabla = (\partial_x, \partial_y)$ and $\widehat{n}$ is a unit vector normal to the boundary $\partial\Omega$. These non-linear equations do not always admit a global solution, see e.g. [19]. A necessary (but not sufficient) condition for a solution to exist is

$$Q = p\times{\rm Area}(\Omega)\;+\;\oint_{\partial\Omega}{\rm d}l\,\gamma'(l) = 0\;. \tag{3}$$

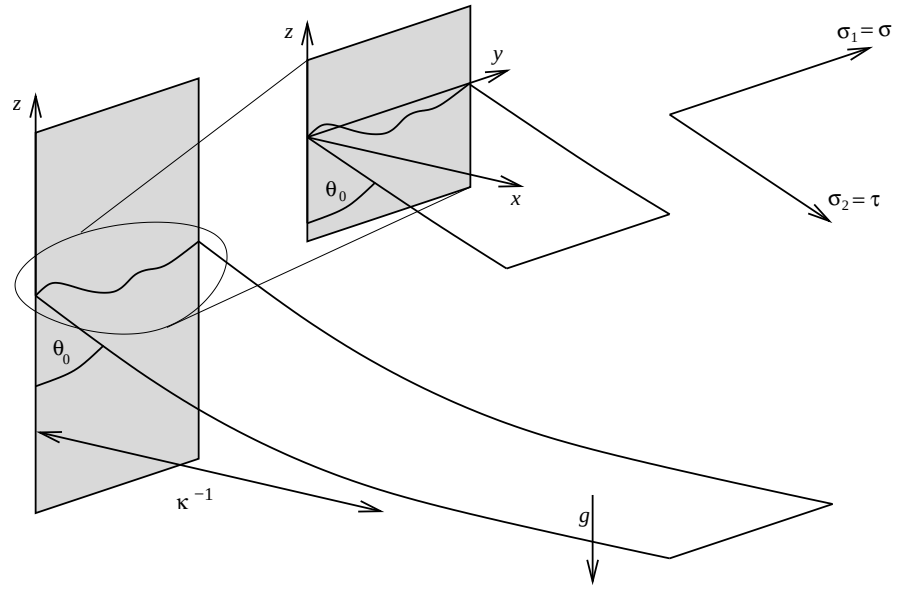

FIG. 1: A fluid surface bounded by a (shaded) planar wall, touching it at the position of a (pinned) contact line. At distances much larger than the capillary length $1/\kappa$, it is flat and perpendicular to the gravitational field (left). Enlargement for distances smaller than $1/\kappa$ (right) which is the range of scales studied here. The unperturbed surface is a plane, making an angle θ_0 with the wall. When perturbed, the conformal parameters (σ_1, σ_2) approach Cartesian coordinates far from the wall, as discussed in section IV.

This is a condition of *average-force cancellation*: indeed, the left-hand side of the above equation couples linearly to the zero mode of $z(x, y)$, and would lead to a runaway solution if it did not vanish, the energy being unbounded in that case. By analogy with string theory we may refer to this as a global tadpole cancellation condition. Note, in particular, that for a homogeneous wall, for which γ' is constant, one must fine tune the ratio of perimeter to area so that it equals p/γ'. If the average-force condition is satisfied, the average height of the fluid surface becomes a free dynamical parameter of the solution, analogous to the string-theoretic *moduli*. Its role must be examined with care as it threatens a priori the stability of any perturbative expansion at weak disorder, and may thus lead to qualitatively new behavior.

The emergence of condition (3) clearly originates from the neglect of gravity. If $g \neq 0$, it is easy to see that the energy is always bounded from below and that the fluid will tend to rise such that $\int \mathrm{d}x\, \mathrm{d}y\, z \simeq Q/\rho g$, the well known capillarity effect. Hence if Q is non zero, one expects that the theory studied here, obtained setting $g = 0$, breaks down for wavevectors $q < \kappa$ (hence especially for the zero mode). However, the interesting point, discussed below, is that if one imposes $Q = 0$ then one can safely set $g = 0$ and obtain a theory which is well defined at all scales. This is the theory studied here. It is illustrated in Fig. 1.

Let us consider minimizing the energy in two steps: We first solve the bulk equations keeping the contact line fixed, i.e. we find the surface of constant mean curvature, $z_h(x, y)$, such that the restriction of z_h to $\partial\Omega$ is a given function $h(l)$. We denote the corresponding bulk energy (or reduced energy functional in the language of [11]) by $E[h] := \mathcal{E}_{\mathrm{bulk}}(z_h)$. The energy of the equilibrium configuration is then the minimum over all contact lines of

$$E[h] - \oint_{\partial\Omega} \gamma'\, h\ . \tag{4}$$

Thus γ' plays the role of a source, and the minimum energy is just the *Legendre transform* of the reduced energy functional. If γ' were to depend also on z, the source would be field-dependent. We will comment on the subtleties of this Legendre transformation between the Dirichlet and Neumann problems in the concluding section.

Let us describe the simplest configuration studied here, which consists of a semi-infinite fluid bounded by a homogeneous planar wall at $x = 0$. We assume from now on that $p = 0$, and that the container at infinity has been adjusted so that the global tadpole condition is satisfied. The unperturbed fluid surface is then an inclined plane, making a contact angle $\theta_0 = \arccos(\gamma'_0/\gamma)$ with the wall, as illustrated in figure 1. We are choosing the origin of coordinates so that the unperturbed fluid surface intersects the wall along $z = 0$, while the perturbed contact line is given by $z = h(y)$. It turns out to be convenient for the following to define:

$$\tilde{E}[h] \ \equiv\ E[h] - E[0] - \gamma \cos\theta_0 \int_y h\ , \tag{5}$$

If the contact line deformations are concentrated in a finite region one expects this energy difference to also be concentrated in a

finite region, and the outer boundaries of the container to decouple. More generally, the simple planar model of figure 1 should give an adequate description of the physics if all other distance scales of the system (including the capillary length, γ/p, and all geometric scales) are much larger than the typical deformation wavelength. We will come back to this subtle issue later on. Note that we have included in the energy difference the contribution, $\mathcal{E}_{\rm bnry}$, of the homogeneous wall. This means that $\tilde{E}[h]$ should start out as a quadratic functional for small $h(y)$.

Let us briefly mention the case of impurity disorder. In this case translation symmetry of the tube is in general broken by the roughness of the wall. The effect of impurities can then be modeled by a variable fluid-solid tension, and the boundary term in (1) becomes:

$$\mathcal{E}_{\rm bnry} \,=\, -\oint_{\partial\Omega} {\rm d}l \int_0^z {\rm d}\zeta\, \gamma'(l,\zeta)\;. \tag{6}$$

The two stage minimization can then be summarized as follows. One writes:

$$\gamma'(l,z) = \gamma'_0(l) + \Delta\gamma'(l,z)\;, \tag{7}$$

where $\gamma'_0(l) = \gamma\cos\theta_0(l)$ is some average or reference value, and defines the shifted functional:

$$\tilde{E}[h] \,\equiv\, E[h] - E[0] - \gamma\oint_{\partial\Omega} {\rm d}l\, \cos\theta_0(l) h(l) \tag{8}$$

Because of disorder the impurities generate a potential for the zero mode z_0 of $z(x,y)$ and the condition (3) cannot hold in general. However we can still impose this condition "on average" $\oint {\rm d}l\, \gamma'_0(l) = 0$ and compute the corresponding $\tilde{E}[h]$. It is this functional which is studied here: it obeys quasi-locality and is well defined for $g = 0$. Once $\tilde{E}[h]$ is known, finding the (equilibrium) position of the contact line amounts to solving in the second stage of the minimization:

$$\min_{h(l)} \left[\tilde{E}[h] - \oint dl \int_0^{h(l)} d\zeta \Delta\gamma'(l,\zeta)\right]\;. \tag{9}$$

This can be viewed as a generalized Legendre transformation, which we will not study here. The aim of this paper being simply to characterize $\tilde{E}[h]$ in presence of an average contact angle. We will use expressions such as pinning condition, or pinned configuration in the following only to denote the fixed-h conditions.

III. CONFORMAL COORDINATES

Computing the area of a minimal surface bounded by a continuous closed curve $\vec{\mathrm{v}}(s)$ is a classical problem of applied mathematics. In this section we will explain how, in conformal gauge, it reduces to a (non-linear and non-local) equation for a function of one variable on the boundary. Let $\vec{r}(\sigma_1,\sigma_2)$ be an arbitrary parameterization of the surface, i.e. $\vec{r} = (x,y,z)$ is the position of the surface Σ corresponding to the values of the two (a priori arbitrarily-chosen) parameters (σ_1,σ_2). We will assume that Σ has the topology of a disk, and that the parameterization is global, i.e. that there is a one-to-one correspondence between points of Σ and points in some parameter domain $\mathcal{D}\subset\mathbb{R}^2$. One should of course keep in mind that, for some boundary curves, these assumptions may have to be relaxed. In terms of the induced metric $g_{ab} = \partial_a\vec{r}\cdot\partial_b\vec{r}$, the area of Σ reads:

$$\mathcal{A} = \iint_{\mathcal{D}} {\rm d}\sigma_1 {\rm d}\sigma_2\, \sqrt{\det g}\;. \tag{10}$$

This expression is invariant under any reparametrization with non-vanishing Jacobian, i.e. $\sigma_1 \to \tilde{\sigma}_1(\sigma_1,\sigma_2)$ and $\sigma_2 \to \tilde{\sigma}_2(\sigma_1,\sigma_2)$ with $\det(\partial_a\tilde{\sigma}_b) \neq 0$. For a surface without 'overhangs' we may use this freedom to set $(\sigma_1,\sigma_2) = (x,y)$, in which case (10) reduces to the expression for the area used in eq. (1). This is a useful parameterization when $\partial_x z$ and $\partial_y z$ are small, but more generally the minimization of the area in this gauge leads to non-linear partial differential equations in two variables, which are hard to solve.

A more convenient choice is conformal coordinates, which are defined implicitly by the two conditions :

$$\partial_1\vec{r}\cdot\partial_2\vec{r} = 0 \quad\text{and}\quad \partial_1\vec{r}\cdot\partial_1\vec{r} = \partial_2\vec{r}\cdot\partial_2\vec{r}\,. \tag{11}$$

Put in words, the two vector fields tangent to the surface are orthogonal everywhere and of equal, not necessarily constant, length. [As the reader can easily verify, the parameterization $(\sigma_1,\sigma_2) = (x,y)$ is conformal only in the special case of constant

z.] It follows from (11) that $g_{ab} = \Phi^2\,\delta_{ab}$, where $\Phi^2 = \partial_1\vec{r}\cdot\partial_1\vec{r}$ is the so-called "conformal factor". Thus in this gauge the area can be written as

$$\mathcal{A} = \frac{1}{2}\iint_{\mathcal{D}} \mathrm{d}\sigma_1\mathrm{d}\sigma_2\,(\partial_1\vec{r}\cdot\partial_1\vec{r} + \partial_2\vec{r}\cdot\partial_2\vec{r})\,, \tag{12}$$

and the variational equations are the Laplace equations in two dimensions :

$$\partial_a\left(\sqrt{\det g}\,g^{ab}\partial_b\,\vec{r}\right) = \left(\partial_1^2+\partial_2^2\right)\vec{r} = 0\,. \tag{13}$$

The embedding coordinates (x,y,z) are therefore harmonic functions of (σ_1,σ_2), and can be written as the real parts of analytic functions of the complex variable $w = (\sigma_1 + i\sigma_2)/2$:

$$x(w,\bar{w}) = 2\,\mathrm{Re}\,X(w)\ \ ,\quad y(w,\bar{w}) = 2\,\mathrm{Re}\,Y(w)\ \ ,\quad z(w,\bar{w}) = 2\,\mathrm{Re}\,Z(w)\ \ . \tag{14}$$

This property of harmonic functions is very special to two dimensions. Our problem is now to determine X, Y and Z for the given boundary curve $\vec{\mathrm{v}}(s)$.

To this end, note first that if the surface is non-singular and bounded, the functions X, Y and Z must be analytic in the interior of the domain $\mathcal{D}$. They are furthermore related by the two conformal-gauge conditions (11), which can be combined in the following equivalent form :

$$(\partial_1 - i\partial_2)\,\vec{r}\cdot(\partial_1 - i\partial_2)\,\vec{r} \;=\; (X')^2 + (Y')^2 + (Z')^2 \;=\; 0\,, \tag{15}$$

where the prime denotes differentiation with respect to w. This rewriting makes manifest the residual freedom of analytic reparametrizations of w. Such complex-analytic changes of coordinates preserve indeed the conformal condition (15), and can be used to map the parameter domain to any convenient simply-connected region in $\mathbb{C}$. Let us assume, for instance, that $\mathcal{D} = \{w\in\mathbb{C}, |w|\le 1\}$ is the unit disk. We write $w = \rho e^{i\phi}$, and denote by $\vec{r}(\phi) := \vec{r}(\phi,\rho=1)$ the boundary curve parameterized by the special conformal coordinate ϕ. Note that $\vec{r}(\phi)$ has a unique harmonic extension to the interior of the disk, and thus determines unambiguously the minimal surface. This follows easily from the fact that the analytic function $X(w)$ admits a Taylor expansion

$$X(w) = \sum_{n=0}^{\infty} X_n w^n\,, \tag{16}$$

so that its restriction to the boundary has no negative-frequency Fourier modes, when identifying $w^n = \mathrm{e}^{i\phi n}$. Thus, to extend $x(\phi)$ to the interior of the disk, we need only split it into positive- and negative-frequency parts, $x(\phi) = x_+(\phi) + x_-(\phi)$. Then x_+ can be extended to $X(w)$ by the replacement $e^{i\phi}\to w$, while $x_- = \bar{x}_+$ extends to the complex-conjugate anti-analytic function $\bar{X}(\bar{w}) = \overline{X(w)}$. If $x(\phi)$ has a zero mode, it must be split equally between the two parts. A simple calculation leads in fact to the following Cauchy relation between $X(w)$ and the boundary restriction of x:

$$X(w) = \frac{1}{4\pi}\int_0^{2\pi}\mathrm{d}\phi'\,x(\phi')\,\frac{e^{i\phi'}+w}{e^{i\phi'}-w}\,. \tag{17}$$

Similar relations hold of course between $Y(w)$ and $y(\phi)$, and also $Z(w)$ and $z(\phi)$. It is, furthermore, easy to check that since $X(e^{i\phi}) = x_+(\phi)$, the conformal-gauge condition (15) is equivalent to

$$\frac{\mathrm{d}\vec{r}_+}{\mathrm{d}\phi}\cdot\frac{\mathrm{d}\vec{r}_+}{\mathrm{d}\phi} = 0 \quad \text{for all } \phi\in[0,2\pi]\,. \tag{18}$$

Let us go back now to the expression (12) for the area. If the surface is minimal, integrating by parts and using Laplace's equation allows to rewrite its area as a boundary integral:

$$\mathcal{A}_{\min} = \frac{1}{2}\int_0^1\rho\mathrm{d}\rho\int_0^{2\pi}\mathrm{d}\phi\,(\partial_\rho\vec{r}\cdot\partial_\rho\vec{r} + \rho^{-2}\partial_\phi\vec{r}\cdot\partial_\phi\vec{r}) \;=\; \frac{1}{2}\int_0^{2\pi}\mathrm{d}\phi\;\vec{r}\cdot\partial_\rho\vec{r}\,\Big|_{\rho=1}\,. \tag{19}$$

The integrand involves the radial derivative of $\vec{r}$, but with the help of Cauchy's equation ($\rho\partial_\rho X = -i\partial_\phi X$, and similarly for the functions Y and Z) we can convert this to an angular derivative, with the result:

$$\mathcal{A}_{\min} \;=\; \frac{i}{2}\int_0^{2\pi}\mathrm{d}\phi\left(\vec{r}_+\cdot\frac{\mathrm{d}\vec{r}_-}{\mathrm{d}\phi} - \vec{r}_-\cdot\frac{\mathrm{d}\vec{r}_+}{\mathrm{d}\phi}\right) \;=\; 2\pi\sum_{n=1}^{\infty} n\,|\vec{r}_n|^2\,. \tag{20}$$

Here $\vec{r}_n$ is the Fourier transform of the function on the circle $\vec{r}(\phi) = \sum_n \vec{r}_n e^{in\phi}$. For later use, we also give two alternative (equivalent) expressions for the minimal area:

$$\mathcal{A}_{\rm min} \,=\, -\frac{1}{4\pi}\int_\phi\int_{\phi'} \frac{{\rm d}\vec{r}}{{\rm d}\phi}\cdot\frac{{\rm d}\vec{r}}{{\rm d}\phi'}\log\sin^2\left(\frac{\phi-\phi'}{2}\right) \,=\, \frac{1}{16\pi}\int_\phi\int_{\phi'} \frac{|\vec{r}(\phi)-\vec{r}(\phi')|^2}{\left(\sin\frac{1}{2}(\phi-\phi')\right)^2}\,. \tag{21}$$

The first can be obtained from eq. (20) by Fourier transform, while the second follows by a double integration by parts and the fact that, thanks to the $i\epsilon$ prescription, only the cross term in the numerator contributes. Note that for suitably smooth $\vec{r}(\phi)$ these integrals are manifestly finite in the $\phi \to \phi'$ region (hence the $i\epsilon$ can be dropped in the final expression - but not if one expands the square).

We have thus succeeded to express the minimal area as an explicit (non-local, but quadratic) functional of $\vec{r}(\phi)$, so one may think that our problem is effectively solved. This is, however, not quite the case, because the transformation from the original parameter of the boundary, to the special conformal coordinate ϕ, depends itself non-trivially on the boundary curve. To make this relation explicit, let us write $s = f(\phi)$, so that $\vec{r}(\phi) = \vec{\rm v}(f(\phi))$. A straightforward calculation starting from the integral expression (17) gives

$$\frac{{\rm d}\vec{r}_+}{{\rm d}\phi} \,=\, -\frac{i}{8\pi}\int {\rm d}\phi'\,\frac{\vec{\rm v}(f(\phi'))}{\sin^2(\frac{\phi-\phi'+i\epsilon}{2})}\,. \tag{22}$$

Plugging this in the gauge condition (18) leads to a non-linear integral equation, that can be used (in principle) to determine $f(\phi)$ for any given boundary curve $\vec{\rm v}(s)$. This is still a non-trivial task, but we have at least reduced the minimal-surface problem to one involving only one unknown function of a single variable. In some cases, the problem can be simplified further by using the residual freedom of conformal transformations to map the unit disk to a suitably-chosen domain. Such is the case when the contact line lies on a plane, as we will now see.

IV. CASE OF A PLANAR WALL

A. The boundary equations

In the configuration of fig. 1 the contact line is restricted to a planar wall, located at $x = 0$. Assuming that it has no overhangs, such a contact line is naturally parameterized by the height function $z = h(y)$. We want to adapt our previous general discussion to this special situation. The story is somewhat simplified by using the convenient conformal coordinates (reminiscent of the proper-time gauge of string theory):

$$X = -ic\,w = -\frac{ic}{2}\,(\sigma + i\tau)\,, \quad \text{so that} \quad x = 2{\rm Re}\,X = c\,\tau\,. \tag{23}$$

Here c is a positive constant, and we have traded (σ_1, σ_2) for the lighter notation (σ, τ). In imposing (23) we have used the residual freedom of conformal transformations, and the fact that X is an analytic function. Note, however, that this choice of gauge might be obstructed globally, as we will explain in appendix A. Since the fluid surface extends out to infinity, the new parameter domain is the upper-half complex plane, $\mathcal{D} = \{w \in \mathbb{C}, {\rm Im}w \geq 0\}$. Later we will consider a second wall at $x = L$, in which case $\mathcal{D}$ will be the infinite strip $0 \leq \tau \leq L/c$. The points at infinity must actually be treated with care: the right procedure is to first make $\mathcal{D}$ finite, by bounding the fluid with outer walls, then move these outer boundaries to infinity.

We will be here interested in surfaces that approach asymptotically the inclined plane

$$\vec{r}_0 = (\sin\theta_0\ \tau,\ \sigma,\ -\cos\theta_0\,\tau)\,. \tag{24}$$

It is therefore convenient to choose $c = \sin\theta_0$, and to define the difference

$$\Delta\vec{r} = \vec{r} - \vec{r}_0\,, \quad \text{with} \quad \Delta\vec{r} \equiv (0, \tilde{y}, \tilde{z})\,. \tag{25}$$

Note that the gauge condition (23) ensures that the first component of $\Delta\vec{r}$ is identically zero. Since the components of both $\vec{r}$ and $\vec{r}_0$ are harmonic, so are those of their difference $\Delta\vec{r}$. We can in fact write $\tilde{y}(w, \bar{w}) = 2{\rm Re}\,\tilde{Y}(w)$ and $\tilde{z}(w, \bar{w}) = 2{\rm Re}\,\tilde{Z}(w)$, where the new analytic functions are given by

$$\tilde{Y} = Y - w\,, \quad \text{and} \quad \tilde{Z} = Z - i\cos\theta_0\,w\,. \tag{26}$$

Following the same logic as in section III, we also define the restrictions of $\tilde{y}$ and $\tilde{z}$ to the real axis, $\tilde{y}(\sigma) \equiv \tilde{y}(\sigma, \tau = 0)$ and $\tilde{z}(\sigma) \equiv \tilde{z}(\sigma, \tau = 0)$. The extension of these functions to the upper-half plane is uniquely determined by the property that they

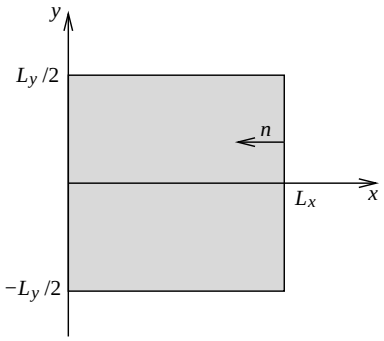

FIG. 2: The domain C and the inward pointing normal.

should be both bounded and harmonic. Indeed, the analytic function $\tilde{Y}$ must have a Fourier-Laplace expansion involving only positive-frequency modes:

$$\tilde{Y}(w) = \int_0^\infty \frac{\mathrm{d}k}{2\pi}\, \tilde{Y}_k\, e^{2ikw} \quad \Longleftrightarrow \quad \tilde{y}(\sigma) = \int_0^\infty \frac{\mathrm{d}k}{2\pi}\, \left(\tilde{Y}_k\, e^{ik\sigma} + c.c.\right) \ , \tag{27}$$

since it would otherwise diverge when $\tau \to \infty$. Thus, to extend $\tilde{y}(\sigma)$ to the upper-half plane, we must first split it into its positive- and negative-frequency parts, $\tilde{y}(\sigma) = \tilde{y}_+(\sigma) + \tilde{y}_-(\sigma)$, then extend $\tilde{y}_+$ analytically and $\tilde{y}_-$ as its complex-conjugate anti-analytic function. The Cauchy integral formula relating $\tilde{Y}(w)$ and $\tilde{y}(\sigma)$ reads

$$\tilde{Y}(w) = \frac{i}{2\pi} \int_{-\infty}^{\infty} \mathrm{d}\sigma\, \frac{\tilde{y}(\sigma)}{2w - \sigma} \ . \tag{28}$$

The right-hand side is analytic in the upper-half complex plane provided that $\tilde{y}(\sigma)$ vanishes at infinity. Of course a similar formula relates also $\tilde{z}(\sigma)$ to its analytic counterpart $\tilde{Z}(w)$.

Our problem is thus reduced to that of finding the two real functions on the real axis, $\tilde{z}(\sigma)$ and $\tilde{y}(\sigma)$. These are related by the pinning condition of the contact line:

$$\tilde{z}(\sigma) = h\Big(\sigma + \tilde{y}(\sigma)\Big) \ . \tag{29}$$

Furthermore, they must obey the conformal constraint (15). After inserting the expressions (26), and using the obvious identities $\tilde{y}_+(\sigma) = \tilde{Y}(\sigma/2)$ and $\tilde{z}_+(\sigma) = \tilde{Z}(\sigma/2)$, this constraint reads:

$$\frac{\mathrm{d}\tilde{y}_+}{\mathrm{d}\sigma} + i\cos\theta_0\, \frac{\mathrm{d}\tilde{z}_+}{\mathrm{d}\sigma} = -\left(\frac{\mathrm{d}\tilde{y}_+}{\mathrm{d}\sigma}\right)^2 - \left(\frac{\mathrm{d}\tilde{z}_+}{\mathrm{d}\sigma}\right)^2 \ . \tag{30}$$

The pair of coupled, non-local equations (29) and (30) is in principle sufficient to determine $\tilde{z}(\sigma)$ and $\tilde{y}(\sigma)$, and hence also the complete shape of the fluid surface. In the following sections we will discuss how to solve these equations numerically, or by a series expansion in powers of $h(y)$. First, however, we must express the energy in terms of the two boundary functions $\tilde{z}(\sigma)$ and $\tilde{y}(\sigma)$.

B. Expression for the energy

The area of an infinite fluid surface is, clearly, infinite. However, for a localized deformation of the contact line, i.e. for $h(y) \to 0$ when $y \to \pm\infty$, we expect the difference in area, $\tilde{\mathcal{A}}_{\min} \equiv \mathcal{A}_{\min}[h] - \mathcal{A}_{\min}[0]$, to be finite. To calculate this difference, we will introduce as a physical cutoff a tubular container $C = \Omega \times \mathbb{R}$, with Ω a rectangle of size $L_x \times L_y$ in the (x, y) plane. We define the associated characteristic function

$$\Theta_C(\vec{r}) := \Theta(x)\,\Theta\left(y + \frac{L_y}{2}\right)\Theta\left(\frac{L_y}{2} - y\right)\Theta(L_x - x) \ = \begin{cases} 1 & \text{if } \ \vec{r} \in C \\ 0 & \text{otherwise} \end{cases}, \tag{31}$$

with $\Theta(a)$ the usual Heaviside step function. The difference of the areas then reads:

$$\tilde{\mathcal{A}}_{\min} = \ \frac{1}{2} \iint_{\mathbb{R}\times\mathbb{R}} \Big[\Theta_C(\vec{r})\, \partial_a\vec{r}\cdot\partial_b\vec{r} \ - \ \Theta_C(\vec{r}_0)\, \partial_a\vec{r}_0\cdot\partial_b\vec{r}_0\Big]\, \delta^{ab} \ , \tag{32}$$

where, after evaluating the right-hand side, we should take the limit $L_x, L_y \to \infty$. Note that cutting off directly the parameter range could give a wrong answer, because the same value of (σ, τ) need not correspond to the same value of (x, y) on the planar and on the deformed surface.

Expanding the integrand of eq. (32) in powers of $\Delta\vec{r}$, and using the fact that

$$\Theta_C(\vec{r}_0 + \Delta\vec{r}) = \Theta_C(\vec{r}_0) + \delta_C(\vec{r}_0)\, \hat{n} \cdot \Delta\vec{r} + \cdots \,, \tag{33}$$

where δ_C is the delta function localized on the boundary of C and $\hat{n}$ is the inward-pointing normal unit vector, leads to the following expression for the area difference:

$$\tilde{\mathcal{A}}_{\min} = \frac{1}{2} \iint_{\mathcal{D}} (\partial_a \Delta\vec{r} \cdot \partial_b \Delta\vec{r} + 2\partial_a \Delta\vec{r} \cdot \partial_b \vec{r}_0)\, \delta^{ab} \; + \int_{\partial\mathcal{D}} |\hat{n} \cdot \partial_\perp \vec{r}_0|^{-1}\, \hat{n} \cdot \Delta\vec{r} + \cdots \;\; . \tag{34}$$

Here $\mathcal{D} = [0, L_x/\sin\theta_0] \times [-L_y/2, L_y/2]$ is the parameter domain defined by the condition $\Theta_C(\vec{r}_0) = 1$, and $\partial\mathcal{D}$ is its boundary. The last term in the above equation accounts for the fact that the cutoff corresponds to a container in physical space, rather than in the space of parameters (σ, τ). The factor $|\hat{n}\cdot\partial_\perp \vec{r}_0|^{-1}$, with $\partial_\perp := \hat{n}\cdot\vec{\partial}$ a derivative in the direction normal to ∂D, is the Jacobian that arises upon converting $\delta_C(\vec{r}_0)$ to a δ-function in parameter space. The neglected terms involve higher powers of $\hat{n}\cdot\Delta\vec{r}$, and one or more partial derivatives. They vanish on the outer boundary, provided $\vec{\Delta} r \to 0$ at infinity, and on the $x = 0$ wall where $\hat{n}\cdot\vec{\Delta} r = 0$ for our choice of gauge. Note that in deriving expression (34) we used the equality $\partial_a \vec{r}_0 \cdot \partial_b \vec{r}_0\, \delta^{ab} = 2$, which follows easily from (24).

Using Stoke's theorem and Laplace's equation we can express all the terms in (34) as boundary integrals,

$$\tilde{\mathcal{A}}_{\min} = \; - \int_{\partial D} \Big(\frac{1}{2} \Delta\vec{r} \cdot \partial_\perp \Delta\vec{r} \; + \Delta\vec{r} \cdot \partial_\perp \vec{r}_0 \; - |\hat{n} \cdot \partial_\perp \vec{r}_0|^{-1}\, \hat{n} \cdot \Delta\vec{r} \Big) \,. \tag{35}$$

Let us consider first the $\sigma = \pm L_y/2$ boundaries: since $\hat{n} = \mp(0, 1, 0)$ there, the last two terms cancel exactly one another, while the term quadratic in $\Delta\vec{r}$ does not contribute as long as $\Delta\vec{r} \to 0$ at infinity. This term does not contribute, for the same reason, at the $\tau = L_x/\sin\theta_0$ boundary. Finally, at both $\tau = 0$ and $\tau = L_x/\sin\theta_0$ we have $\hat{n}\cdot\Delta\vec{r} = 0$, since $\hat{n} = \pm(1, 0, 0)$ on these boundaries and, with our choice of gauge, $\Delta\vec{r} = (0, \tilde{y}, \tilde{z})$. Putting all these facts together we obtain:

$$\tilde{\mathcal{A}}_{\min} = \; \int_{-\infty}^{\infty} \mathrm{d}\sigma \, \Big\{ -\frac{1}{2} (\tilde{y}\, \partial_\tau \tilde{y} + \tilde{z}\, \partial_\tau \tilde{z}) \Big|_{\tau=0} \; + \cos\theta_0\, \tilde{z} \Big|_{\tau=0} - \cos\theta_0\, \tilde{z} \Big|_{\tau = L_x/\sin\theta_0} \Big\} \,, \tag{36}$$

where the limit $L_y \to \infty$ has already been taken on the right-hand-side. The τ-derivatives in the first term can be converted to σ-derivatives with the help of the Cauchy equation. As for the last two linear terms, they cancel because $\tilde{z}$ is harmonic (both are proportional to the same $k = 0$ Fourier mode). Thus the difference of the areas reads:

$$\tilde{\mathcal{A}}_{\min} = \; \frac{1}{2} \int_{-\infty}^{\infty} \mathrm{d}\sigma \, \Big[i\tilde{y}_+ \frac{\mathrm{d}\tilde{y}_-}{\mathrm{d}\sigma} + i\tilde{z}_+ \frac{\mathrm{d}\tilde{z}_-}{\mathrm{d}\sigma} \; + \; c.c. \Big] \,. \tag{37}$$

Although this calculation is correct, the cancellation of the linear terms is, from the physical point of view, rather misleading. It involves two opposite walls which are infinitely far apart in the $L_x \to \infty$ limit, and looks therefore highly non-local. A physically more significant cancellation occurs in the energy functional $\tilde{E}[h]$, which (as explained in section II) receives a contribution from the fluid-solid interface:

$$\mathcal{E}_{\mathrm{bnry}} \; = \; - \oint_{\partial\mathcal{D}} \mathrm{d}l\, \gamma'\, \tilde{z} \; = \; -\gamma \cos\theta_0 \int_{-\infty}^{\infty} \mathrm{d}\sigma \, \Big\{ \tilde{z}(1 + \partial_\sigma \tilde{y}) \Big|_{\tau=0} - \tilde{z} \Big|_{\tau = L_x/\sin\theta_0} \Big\} \;\; . \tag{38}$$

The second equality can be understood as follows: the unperturbed planar surface meets the $x = 0$, $x = L_x$ and $y = \pm L_y/2$ walls at angles equal to θ_0 , $\pi - \theta_0$ and $\pi/2$, respectively. Young's equilibrium condition thus requires that, in the absence of impurities:

$$\gamma' = \begin{cases} \gamma\cos\theta_0 & \text{for} \;\; x = 0 \,, \\ 0 & \text{for} \;\; y = \pm L_y/2 \,, \\ -\gamma\cos\theta_0 & \text{for} \;\; x = L_x \;\; . \end{cases} \tag{39}$$

Furthermore, along the first and the last wall the invariant length is $\mathrm{d}l = \mathrm{d}y = (1 + \partial_\sigma \tilde{y})\, \mathrm{d}\sigma$. Dropping the quadratic term at $x = L_x$, since both $\tilde{y}$ and $\tilde{z}$ must tend there to zero, gives the advertised equation (38). Adding this to $\gamma\tilde{\mathcal{A}}_{\min}$ leads to our final expression for the energy:

$$\tilde{E}[h] = \; \frac{\gamma}{2} \int_{-\infty}^{\infty} \mathrm{d}\sigma \, \Big[i\tilde{y}_+ \frac{\mathrm{d}\tilde{y}_-}{\mathrm{d}\sigma} + i\tilde{z}_+ \frac{\mathrm{d}\tilde{z}_-}{\mathrm{d}\sigma} - \cos\theta_0\, \tilde{z} \frac{\mathrm{d}\tilde{y}}{\mathrm{d}\sigma} \; + \; c.c. \Big] \,. \tag{40}$$

Note that the linear terms cancel here separately on each wall, and that all the contributions to the energy are "quasi-local". Thus the large-volume cutoff decouples, as expected, in the calculation of the energy (but not of the separate contributions $\gamma\tilde{\mathcal{A}}_{\rm min}$ and $\mathcal{E}_{\rm bnry}$). The only restriction on the cutoff is that it should not destabilize the unperturbed planar surface. We confirm these claims by a calculation in appendix B, which includes as an extra control parameter the inclination angle of the outer wall.

For later use, we will also need the expression of the energy in terms of the Fourier components of $\tilde{y}(\sigma)$ and $\tilde{z}(\sigma)$. Using eq. (27), and doing some straightforward algebra leads to

$$\tilde{E}[h] = \gamma \int_0^\infty \frac{\mathrm{d}k}{2\pi}\, k \left(|\tilde{Y}_k + i\cos\theta_0 \tilde{Z}_k|^2 + \sin^2\theta_0\, |\tilde{Z}_k|^2 \right) . \tag{41}$$

Note that the energy is quadratic in $\tilde{y}$ and $\tilde{z}$, where the function $y(\sigma) = \sigma + \tilde{y}(\sigma)$ relates the natural parameterization of the contact line, to the conformal parameterization in terms of σ. As was explained in the previous section, the problem is non-linear because this change of coordinate depends explicitly on the pinning profile.

V. PERTURBATIVE EXPANSION

The pair of equations (29) and (30) cannot be solved, in general, in closed form. However, if the contact line is deformed only "slightly" (this will be made more precise later), then $\tilde{y}$ and $\tilde{z}$ should both be small. We may therefore expand the right-hand side of eq. (29) in a Taylor series,

$$\tilde{z}(\sigma) \;=\; \sum_{n=0}^{\infty} \frac{\mathrm{d}^n h(\sigma)}{\mathrm{d}\sigma^n}\, \frac{\tilde{y}(\sigma)^n}{n!} \;, \tag{42}$$

where both $\tilde{y}$ and the derivatives of h are now evaluated at the argument σ. Furthermore, solving the quadratic equation (30) for $\mathrm{d}\tilde{y}_+/\mathrm{d}\sigma$ and integrating gives:

$$\tilde{y}_+(\sigma) = \int_{-\infty}^{\sigma} \mathrm{d}\sigma' \left\{ \left[\frac{1}{4} - \Big(\frac{\mathrm{d}\tilde{z}_+}{\mathrm{d}\sigma'}\Big)^2 - i\cos\theta_0 \frac{\mathrm{d}\tilde{z}_+}{\mathrm{d}\sigma'} \right]^{1/2} - \frac{1}{2} \right\} \;. \tag{43}$$

Note that we have picked the solution of the quadratic equation that vanishes for $\tilde{z}_+ \to 0$, and we have also fixed arbitrarily the irrelevant (complex) integration constant. Since $\tilde{z}$ is small, we may expand the integrand on the right-hand side to find

$$\begin{aligned} \tilde{y}_+(\sigma) &= \sum_{n=1}^{\infty} \frac{2^{n-1}}{n!} \left[(-1)\cdot 1\cdot 3\cdot 5 \cdots (2n-3)\right] \times \int_{-\infty}^{\sigma} \mathrm{d}\sigma' \left[\Big(\frac{\mathrm{d}\tilde{z}_+}{\mathrm{d}\sigma'}\Big)^2 + i\cos\theta_0 \frac{\mathrm{d}\tilde{z}_+}{\mathrm{d}\sigma'} \right]^n \\ &= \int_{-\infty}^{\sigma} \mathrm{d}\sigma' \left[-i\cos\theta_0 \frac{\mathrm{d}\tilde{z}_+}{\mathrm{d}\sigma'} \;-\; \sin^2\theta_0 \Big(\frac{\mathrm{d}\tilde{z}_+}{\mathrm{d}\sigma'}\Big)^2 \;+\; \cdots \right] \end{aligned} \tag{44}$$

Equations (42) and (44) can now be solved iteratively as follows: one starts with the lowest-order solution of the first equation, $\tilde{z}(\sigma) = h(\sigma)$, and inserts it into the second one to find $\tilde{y}_+ = -i\cos\theta_0\, h_+$. Inserting the result in eq. (42) gives $\tilde{z}$ at quadratic order in h, and from eq. (44) we can obtain $\tilde{y}$ to the same order. Iterating the procedure gives, in principle, the solution to any desired order in the pinning profile h.

In order to write the answer in a compact form, we introduce the following notation. If $f_\pm(\sigma)$ are the positive- and negative-frequency parts of any real function $f(\sigma)$, then

$$f \equiv f_+ + f_- \quad \text{and} \quad i\,\widehat{f} := f_+ - f_- \;, \tag{45}$$

where the second equality defines the *dual* function $\widehat{f}(\sigma)$. Note that f and $\widehat{f}$ are both real – this follows from the fact that $f_- = (f_+)^*$. Now the first few orders in the expansion of the solution read:

$$\tilde{z} = h \;+\; \cos\theta_0 \frac{\mathrm{d}h}{\mathrm{d}\sigma}\,\widehat{h} \;+\; \frac{\cos^2\theta_0}{2}\frac{\mathrm{d}^2 h}{\mathrm{d}\sigma^2}\,\widehat{h}^2 \;-\; \frac{\mathrm{d}h}{\mathrm{d}\sigma}\left[\sin^2\theta_0 \int_{-\infty}^{\sigma} \Big(\frac{\mathrm{d}h_+}{\mathrm{d}\sigma'}\Big)^2 \mathrm{d}\sigma' + i\cos^2\theta_0 \Big(\frac{\mathrm{d}h}{\mathrm{d}\sigma}\widehat{h}\Big)_+ + \,c.c.\right] + O(h^4) \,, \tag{46}$$

$$\tilde{y}_+ = -i\cos\theta_0\, h_+ \;-\; \sin^2\theta_0 \int_{-\infty}^{\sigma} \Big(\frac{\mathrm{d}h_+}{\mathrm{d}\sigma'}\Big)^2 \mathrm{d}\sigma' - i\cos^2\theta_0 \Big(\frac{\mathrm{d}h}{\mathrm{d}\sigma}\widehat{h}\Big)_+ \;+\; O(h^3) \,, \tag{47}$$

where we have stopped at one order lower in the expansion of $\tilde{y}$ for a reason that will become apparent in a minute. It will be useful to have also at hand the Fourier transforms of these expressions. Noting that

$$f_+ g_+ + f_- g_- = \frac{1}{2}(fg - \widehat{f}\,\widehat{g}) \quad \text{and} \quad i\,\widehat{f}_k = f_k\,\frac{k}{|k|} \;, \tag{48}$$

we find after some straightforward manipulations:

$$i\tilde{Y}_k \;=\; h_k\,\cos\theta_0 \;+\int h_{k_1}h_{k_2}\,k_1k_2\,\Big[\,\frac{\sin^2\theta_0}{k}\,\Theta(k_1k_2)+\,\frac{\cos^2\theta_0}{|k_2|}\Big]\;+\;O(h^3)\;, \tag{49}$$

$$\begin{aligned}\tilde{Z}_k \;=\; h_k &+\int h_{k_1}h_{k_2}\,k_1k_2\,\frac{\cos\theta_0}{|k_2|}\\ &+\int h_{k_1}h_{k_2}h_{k_3}\,k_1k_2k_3\,\Big[\,\frac{\sin^2\theta_0}{k_2+k_3}\,\Theta(k_2k_3)+\frac{\cos^2\theta_0\,k_1}{2|k_2k_3|}+\frac{\cos^2\theta_0\,(k_2+k_3)}{|k_3||k_2+k_3|}\Big]+\;O(h^4)\;.\end{aligned} \tag{50}$$

Here the integrals run over all k_j, with normalization $\int \mathrm{d}k_j/(2\pi)$ and the condition that $\sum k_j = k$. The step functions $\Theta(k_ik_j)$ force the two momenta to have the same sign, and we have assumed that k is positive. Recall that $\tilde{Y}_k$ enters into the expression (41) for the energy through the combination

$$i(\tilde{Y}_k + i\cos\theta_0\,\tilde{Z}_k) \;=\; \frac{\sin^2\theta_0}{k}\;\int h_{k_1}h_{k_2}\,k_1k_2\,\Theta(k_1k_2)\;+\;O(h^3)\;. \tag{51}$$

Since this starts out quadratically in h, the cubic corrections contribute to the energy at $O(h^5)$. This explains why we have truncated the expansion of $\tilde{y}$ at one order lower than the expansion of $\tilde{z}$.

Inserting (50) and (51) in (41), and doing some straightforward manipulations, leads to the following expression for the energy of the deformed contact line at quartic order:

$$\tilde{E}[h] = E_2 + E_3 + E_4 \;+\; O(h^5)\;,$$

where

$$E_2 = \gamma\sin^2\theta_0\int_0^\infty\frac{\mathrm{d}k}{2\pi}\,k\,|h_k|^2\;\;, \tag{52}$$

$$E_3 = \gamma\cos\theta_0\;\sin^2\theta_0\int h_{k_1}h_{k_2}h_{k_3}\,\frac{|k_1|k_2k_3}{|k_3|}\equiv-\gamma\cos\theta_0\;\sin^2\theta_0\int h_{k_1}h_{k_2}h_{k_3}\,k_1k_2\,\Theta(k_1k_2) \tag{53}$$

$$\begin{aligned}E_4 = \frac{\gamma}{2}\int h_{k_1}h_{k_2}h_{k_3}h_{k_4}\,k_1k_2k_3k_4\,\Bigg[&\sin^4\theta_0\,\Big\{\frac{\Theta(k_1k_2)\Theta(k_3k_4)}{|k_1+k_2|}+\frac{2k_1}{|k_1|}\frac{\Theta(k_3k_4)}{(k_3+k_4)}\Big\}\\ &+\sin^2\theta_0\cos^2\theta_0\,\Big\{\frac{k_1k_4}{|k_2k_3k_4|}+\frac{{k_2}^2-{k_1}^2}{|k_1||k_4||k_1+k_2|}\Big\}\Bigg]\;.\end{aligned} \tag{54}$$

The integrals in (53) and (54) run over all k_j with the condition that $\sum k_j = 0$. As a check, note that for $\theta_0 = \pi/2$ the energy is invariant under reflection, $h \to -h$, of the contact line. Note also that the expressions multiplying $\prod h_{k_j}$ inside the integrals are invariant under the combination of complex conjugation and change of sign of all the momenta, consistently with the fact that $\tilde{E}[h]$ should be real. The expression for E_3 agrees with the one derived in [12] by a different method.

The Joanny-de Gennes linear theory [10] corresponds to the leading term of the above expansion. Comparing E_2 with the energy of an elastic rod, $E \sim \int k^2|h_k|^2$, one notes a softening of short-distance modes, and corresponding hardening of long-distance modes, due to the interactions mediated by the surface. In real space, the JdG energy can be written as (see the discussion in section III):

$$E_2 \;=\; \frac{\gamma}{4\pi}\;\sin^2\theta_0\iint\,d\sigma d\sigma'\frac{[h(\sigma)-h(\sigma')]^2}{(\sigma-\sigma'+i\epsilon)^2}\;. \tag{55}$$

This quadratic, non-local functional has appeared in a variety of other contexts, e.g. in simple models of quantum-mechanical dissipation [20, 21]. Note that E_2 is invariant under SL(2,$\mathbb{R}$) transformations, i.e. under conformal transformations that preserve the upper-half complex plane, $\sigma \to \frac{a\sigma+b}{c\sigma+d}$, $h \to h$, with a, b, c, d real and $ad-bc=1$. The full energy is not only translationally-invariant, but it also transforms covariantly under rescalings of the physical space:

$$\tilde{E}[h^{(\lambda)}] \;=\; \lambda^2\,\tilde{E}[h] \qquad \text{if} \qquad h^{(\lambda)}(y) \equiv \lambda\,h(\lambda^{-1}y)\;\;. \tag{56}$$

This implies that the perturbative expansion is really an expansion in derivatives, as should be expected from the fact that the classical problem has no intrinsic length scale. We will return to this point later on.

It will be useful, for comparison with the following section, to rewrite the quartic contributions to the energy differently. First, we note that the two terms multiplying $\sin^4\theta_0$ are equal up to a factor of -2. This follows from the following chain of replacements, which are allowed upon symmetrization of the integrand:

$$\frac{2k_1}{|k_1|}\frac{\Theta(k_3k_4)}{(k_3+k_4)} \quad\longrightarrow\quad -(s_1+s_2)\,\frac{\Theta(k_3k_4)}{(k_1+k_2)} \quad\longrightarrow\quad -(1+s_1s_2)\,\frac{\Theta(k_3k_4)}{|k_1+k_2|}$$

Here $s_j = k_j/|k_j|$ is the sign of the momentum k_j, and in the second step we have used the fact that the sign of (k_1+k_2) is the same as the sign of either k_1 or k_2, since the expression is multiplied by $(1+s_1s_2) = 2\Theta(k_1k_2)$. Likewise, one can justify the following replacement:

$$\frac{k_1}{|k_1|}\frac{\Theta(k_3k_4)}{(k_3+k_4)} \quad\longrightarrow\quad \frac{k_1k_4}{|k_1||k_4||k_1+k_2|}\,, \quad\text{and}\quad \frac{{k_2}^2-{k_1}^2}{|k_1||k_4||k_1+k_2|} \quad\longrightarrow\quad \frac{({k_2}^2+{k_3}^2)-({k_1}^2+{k_4}^2)}{2|k_1||k_4||k_1+k_2|}\,.$$

Putting all these facts together, using that $\sum_j k_j = 0$ and doing some straightforward rearrangements leads to the following alternative expression for the quartic energy:

$$E_4 = \frac{\gamma}{2}\sin^2\theta_0\int\prod_{j=1}^{4}(k_j h_{k_j})\left[-\frac{\Theta(k_1k_2)\Theta(k_3k_4)}{|k_1+k_2|}+\cos^2\theta_0\left\{\frac{k_1k_4}{|k_2k_3k_4|}-\frac{k_2k_3}{|k_1||k_4||k_1+k_2|}\right\}\right]. \tag{57}$$

This somewhat more economical expression will be easier to compare with the diagrammatic expansion, to which we will now turn our attention. Note that the expression for E_4 in the particular case $\theta_0 = \pi/2$ was also found in [13] using the perturbative solution of the non-linear equation (not using conformal coordinates). It is possible, though cumbersome, to extend the method to arbitrary θ_0 [22].

VI. DIAGRAMMATIC METHOD

The perturbative expansion of the energy can be organized efficiently by using a Lagrange-multiplier field to impose the pinning constraint of the contact line. One starts with the following variational principle for the area:

$$\mathcal{A}_{\min} \;=\; \operatorname{extr}\mathcal{A}(\alpha,\vec{r})\,, \quad\text{with}\quad \mathcal{A}(\alpha,\vec{r}) = \iint_{\mathcal{D}}\mathrm{d}^2\sigma\sqrt{\det g} \;-\; \int_{\partial\mathcal{D}}\mathrm{d}s\,\alpha(s)\Big[z(s)-h\big(y(s)\big)\Big]\,. \tag{58}$$

Here s parameterizes the boundary of the domain $\mathcal{D}$, and α is a Lagrange-multiplier field that transforms under reparametrizations such that $\alpha(s)\,\mathrm{d}s$ remains unchanged. Since $\mathcal{A}(\alpha,\vec{r})$ is reparametrization-invariant, we are free to choose the conformal gauge and to set $x = \sin\theta_0\,\tau$ as before. Thus $\mathcal{D}$ is the upper-half plane $\tau \geq 0$, and we may choose $s = \sigma$ for the boundary parameter. We also define $y = \sigma + \tilde{y}$ and $z = -\cos\theta_0\,\tau + \tilde{z}$, and we subtract from $\mathcal{A}$ the area of the flat fluid surface. This gives $\tilde{\mathcal{A}}_{\min} \;=\; \operatorname{extr}\tilde{\mathcal{A}}$, where

$$\tilde{\mathcal{A}}(\alpha,\tilde{y},\tilde{z}) = \frac{1}{2}\iint_{\tau\geq 0}(\partial_a\tilde{y}\,\partial^a\tilde{y}+\partial_a\tilde{z}\,\partial^a\tilde{z}) \;-\; \int_{\tau=0}\Big[\alpha\left(\tilde{z}-h(\sigma+\tilde{y})\right) \;-\; \cos\theta_0\,\tilde{z}\Big]\,. \tag{59}$$

The last term in the above expression comes from the cross term $\partial_a z_0\,\partial^a\tilde{z} \;=\; -\cos\theta_0\,\partial_\tau\tilde{z}$ in the area difference. This is a total derivative, which is why it only contributes a boundary term. Note that, in the light of our discussion in section IV, all contributions from the boundaries at infinity have been dropped. This is legitimate since we are ultimately interested in the energy (40) rather than in the area of the fluid surface. Alternatively, one can view $\tilde{\mathcal{A}}(\alpha,\vec{r})$ as an action and consider the path integral over the fields $\vec{r}$ and α [28]. Since we are doing only a tree level calculation there is no need to worry about Fadeev-Popov ghosts, which would be important for the study of thermal or quantum fluctuations. Fluctuating surfaces [23] are beyond the scope of the present study.

It looks, at first sight, rather odd that in the above formulation the conformal-gauge conditions are not explicitly imposed. The extrema of $\tilde{\mathcal{A}}(\alpha,\tilde{y},\tilde{z})$ should therefore obey these conditions automatically. To see why, note that the variation of (59) leads to the boundary equations:

$$\partial_\tau\tilde{y} = \alpha(\sigma)\,h'(\sigma+\tilde{y}) \quad\text{and}\quad \partial_\tau\tilde{z} = -\alpha(\sigma)+\cos\theta_0 \quad\text{at}\quad \tau = 0\,. \tag{60}$$

From the above boundary equations, and from the pinning constraint $z = h(y)$, we deduce:

$$\partial_\tau\vec{r} \;=\; \big(\sin\theta_0\,,\,\alpha(\sigma)\,h'(y)\,,\,-\alpha(\sigma)\big) \quad\text{and}\quad \partial_\sigma\vec{r} \;=\; \big(0\,,\,\partial_\sigma y\,,\,h'(y)\,\partial_\sigma y\big)\,. \tag{61}$$

Thus, on the boundary, the condition $\partial_\sigma \vec{r}\cdot\partial_\tau \vec{r} = 0$ holds. This implies that the function $\partial_w \vec{r}\cdot\partial_w \vec{r}$, which is analytic in the upper half plane and vanishes at infinity, has zero imaginary part on the real axis. From the Cauchy-Poisson integral formula [24] we conclude that it vanishes everywhere, so that the conformal gauge conditions (15) are indeed satisfied.

In order to develop simple diagrammatic rules, we first solve the harmonic equation for the "bulk" fields keeping their restrictions to the boundary, $\tilde{y}(\sigma) := \tilde{y}(\sigma, 0)$ and $\tilde{z}(\sigma) := \tilde{z}(\sigma, 0)$, fixed. As has been already discussed, this leads to the replacement

$$\frac{1}{2}\iint_{\tau\geq 0} \partial_a\tilde{y}\,\partial^a\tilde{y} \;\;\longrightarrow\;\; \frac{i}{2}\int_{\tau=0}(\tilde{y}_+\frac{\mathrm{d}\tilde{y}_-}{\mathrm{d}\sigma} - \tilde{y}_-\frac{\mathrm{d}\tilde{y}_+}{\mathrm{d}\sigma}) \;=\; \frac{1}{2}\int_k |k|\,\tilde{y}_k\,\tilde{y}_{-k}\;\;, \tag{62}$$

and likewise for the field $\tilde{z}$. Next, we solve the linear equations for $\tilde{z}(\sigma)$, thus eliminating it entirely from the expression (59). The new variational functional, expressed in terms of Fourier components, reads

$$\tilde{\mathcal{A}}(\alpha,\tilde{y}) \;=\; \frac{1}{2}\int_k |k|\,\tilde{y}_k\,\tilde{y}_{-k} \;-\; \frac{1}{2}\int_k \frac{1}{|k|}\,\delta\alpha_k\,\delta\alpha_{-k} \;+\; \int_k \alpha_{-k}H_k\;, \tag{63}$$

where $\alpha_k = \cos\theta_0\, 2\pi\delta(k) + \delta\alpha_k$, and H_k is the Fourier transform of $H(\sigma) = h(\sigma + \tilde{y}(\sigma))$. This result also follows if one uses the path integral formulation and integrates over the fields $\tilde{y}$ and $\tilde{z}$ in the bulk. More explicitly

$$H_k = h_k + \int ik_1\,h_{k_1}\,\tilde{y}_{k_2} + \frac{1}{2}\int (ik_1)^2 h_{k_1}\,\tilde{y}_{k_2}\,\tilde{y}_{k_3} + \cdots\;\;, \tag{64}$$

where the integrals run over $\sum k_j = k$. The extremum of the functional (63) can be computed by summing tree-level diagrams of a 1-dimensional field theory. The 1-point function and propagators read:

$$\begin{aligned} \text{—}\!\!\subset\!\!\text{—} \;&:=\; \langle\,\alpha_k\,\rangle \;=\; \cos\theta_0\,2\pi\delta(k) \\ \text{———} \;&:=\; \langle\,\delta\alpha_k\,\delta\alpha_{-k}\,\rangle \;=\; |k| \\ \sim\!\sim\!\sim \;&:=\; \langle\tilde{y}_k\,\tilde{y}_{-k}\rangle \;=\; -\frac{1}{|k|} \end{aligned} \tag{65}$$

while the first few vertices, deriving from the last term of (63), are as follows:

(66)

Note that all of these vertices are proportional to the amplitude of the pinning profile. Furthermore wiggly lines, corresponding to the field $\tilde{y}$, can only terminate on another vertex in a vacuum tree diagram. Thus only a finite number of vertices contributes to a given order in the expansion in h. Solid lines corresponding to the Lagrange-multiplier field α may end at the tadpole $\langle\alpha_k\rangle = \cos\theta_0\,2\pi\delta(k)$, which carries no extra power of h. Note also that at the vertices momentum is injected by h_k, which has to be taken into account for momentum conservation.

Using the above diagrammatic rules, one can compute any desired order in the expansion of $\tilde{E}[h]$. This is obtained by multiplying the extremum of (63) with γ, and then subtracting the linear contribution of the wall, $\mathcal{E}_{\mathrm{bnry}} = \gamma'\int h = \gamma\cos\theta_0\,h_0$ (see section IV). This contribution cancels precisely the tadpole diagram

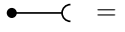

(67)

in agreement with the fact that the unperturbed, planar fluid surface should be stable. Denoting by E_n the nth-order term in the perturbative expansion of $\tilde{E}[h]$ one finds:

Order 2:

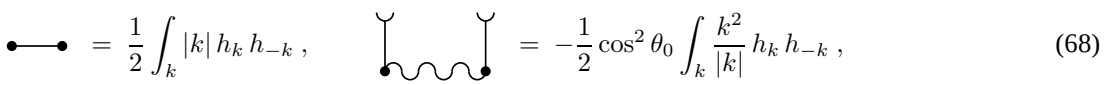

(68)

so that

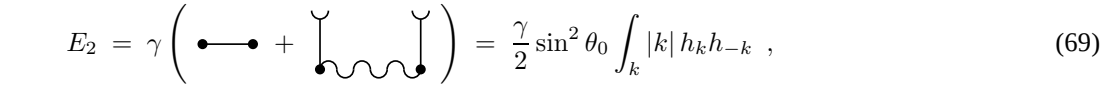

(69)

which is precisely the Joanny-de Gennes quadratic energy.

Order 3:

$$= \cos\theta_0 \int \frac{|k_1|k_2k_3}{|k_3|}\, h_{k_1} h_{k_2} h_{k_3} \tag{70}$$

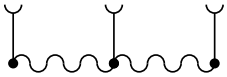

$$= \frac{1}{2}\cos^3\theta_0 \int \frac{k_1 {k_2}^2 k_3}{|k_1||k_3|}\, h_{k_1} h_{k_2} h_{k_3} \tag{71}$$

These two contributions are of the same form. To see why, one must symmetrize the integrands over all permutations of [123], and then use the identities that follow from momentum conservation:

$$\frac{1}{2}\, s_1 s_3\, {k_2}^2 + \text{perms} \;=\; s_1 s_3\, ({k_1}^2 + k_1 k_3) + \text{perms} \;=\; -s_1 s_3\, k_1 k_2 + \text{perms}\,,$$

where $s_j = k_j/|k_j|$ is the sign of k_j. Thus, the sum of the two diagrams gives

$$E_3 \;=\; \gamma \left(\quad + \quad \right) \;=\; \gamma \cos\theta_0\, \sin^2\theta_0 \int \frac{|k_1|k_2k_3}{|k_3|}\, h_{k_1} h_{k_2} h_{k_3}\,, \tag{72}$$

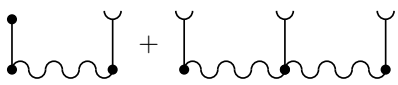

which agrees with the calculation (53) of the previous section.

Order 4:

$$= \frac{1}{2} \int \frac{|k_1|k_2k_3|k_4|}{|k_1+k_2|} h_{k_1} h_{k_2} h_{k_3} h_{k_4} \tag{73}$$

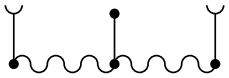

$$= \frac{1}{2}\cos^2\theta_0 \int \frac{k_1 k_2^2 k_3|k_4|}{|k_1||k_3|}\, h_{k_1} h_{k_2} h_{k_3} h_{k_4} \tag{74}$$

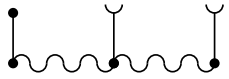

$$= \cos^2\theta_0 \int \frac{k_1 k_2^2 k_3|k_4|}{|k_1|\,|k_1+k_2|}\, h_{k_1} h_{k_2} h_{k_3} h_{k_4} \tag{75}$$

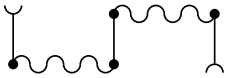

$$= \frac{1}{2}\cos^2\theta_0 \int \frac{k_1k_2k_3k_4|k_1+k_2|}{|k_1||k_4|}\, h_{k_1} h_{k_2} h_{k_3} h_{k_4} \tag{76}$$

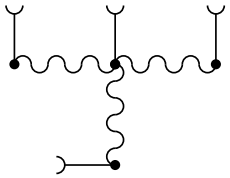

$$= \frac{1}{6}\cos^4\theta_0 \int \frac{k_1k_2k_3k_4^3}{|k_1||k_2||k_3|}\, h_{k_1} h_{k_2} h_{k_3} h_{k_4} \tag{77}$$

$$= \frac{1}{2}\cos^4\theta_0 \int \frac{k_1 k_2^2 k_3^2 k_4}{|k_1||k_1+k_2||k_4|}\, h_{k_1} h_{k_2} h_{k_3} h_{k_4} \tag{78}$$

Note that the power of $\cos\theta_0$ corresponds to the number of "hooks" of a given diagram. For $\cos\theta_0 = 0$ only the first of these diagrams contributes. Using the replacements

$$\frac{s_1 s_4}{|k_1+k_2|} \;\longrightarrow\; \frac{(s_1+s_2)(s_3+s_4)}{4|k_1+k_2|} \;=\; -\frac{\Theta(k_1k_2)\Theta(k_3k_4)}{|k_1+k_2|}\,,$$

one can check that this diagram agrees with our previous result (57). To show that the expression (57) also agrees with $E_4 = \gamma\,[(73)+(74)+(75)+(76)+(77)+(78)]$ for arbitary contact angle θ_0 we proceed as follows: first diagrams (74) and (77)

can be combined to reproduce the second term in (57). To see why, one must replace $\frac{1}{3}k_4{}^2 = -\frac{1}{3}k_4(k_1+k_2+k_3) \rightarrow -k_1k_4$ in the integrand of the diagram (77). Secondly, one can show that for $\cos\theta_0 = 1$ the sum of the remaining diagrams, $(73)+(75)+(76)+(78)$, is exactly zero. Indeed, writing the integrands of these diagrams in the order of their appearance we find:

$$\frac{k_1k_2k_3k_4}{|k_1|\,|k_4|\,|k_1+k_2|}\left[k_1k_4+2k_2k_4+(k_1+k_2)^2+k_2k_3\right] = \frac{k_1k_2k_3k_4}{|k_1|\,|k_4|\,|k_1+k_2|}\left[k_1k_4+2k_2k_4-(k_1+k_2)(k_3+k_4)+k_2k_3\right]$$
$$= \frac{k_1k_2k_3k_4}{|k_1|\,|k_4|\,|k_1+k_2|}\,(k_2k_4-k_1k_3) = \frac{k_1k_2k_3k_4}{|k_1|\,|k_4|\,|k_3+k_4|}\,(k_2k_4-k_1k_3)\ , \tag{79}$$

where in the first and the third equality we have used the conservation of momentum. Since the last two expressions are equal they can be replaced by their average. The result is antisymmetric under the exchange of 1 with 4 and 2 with 3, so after multiplication with $h_{k_1}h_{k_2}h_{k_3}h_{k_4}$ it gives zero as claimed. We are thus free to subtract this vanishing expression times $\frac{1}{2}\cos^2\theta_0$ from the sum of all diagrams. This removes the contributions (75) and (76), and changes the coefficients of (73) and (78) to those of the corresponding terms in (57). This completes the proof that equation (57) agrees with the diagrammatic calculation of the energy.

The diagrammatic expansion can be extended to higher orders. As an illustration, let us consider the case of a perpendicular contact angle, in which case the tadpole vanishes. The symmetry under $h \rightarrow -h$ guarantees that only even powers appear in the expansion of $E[h]$. The sixth and eighth order terms are given by:

$$E_6\Big|_{\theta_0=\pi/2} = \gamma$$  $$= \gamma \int \frac{|k_1|k_2k_3^2|k_4|k_5|k_6|}{|k_1+k_2||k_5+k_6|}\prod_{j=1}^{6} h_{k_j} \tag{80}$$

$$E_8\Big|_{\theta_0=\pi/2} = \gamma\,\Big($$ 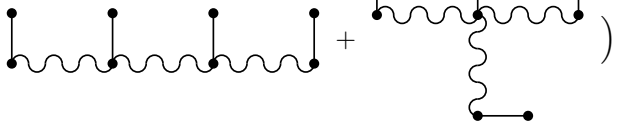

where  $$= \int \frac{|k_1|\,k_2k_3^2\,|k_4|\,k_5^2\,|k_6|\,k_7\,|k_8|}{|k_1+k_2||k_1+k_2+k_3+k_4||k_7+k_8|}\prod_{j=1}^{8} h_{k_j} \tag{81}$$

and 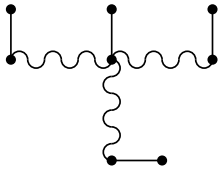 $$= \int \frac{|k_1|\,k_2\,|k_3|\,k_4\,|k_5|\,k_6\,|k_7|\,k_8^3}{|k_1+k_2||k_3+k_4||k_5+k_6|}\prod_{j=1}^{8} h_{k_j} \tag{82}$$

We will comment further on these results in the final section.

VII. NUMERICAL ALGORITHM

As was shown in section IV, the problem of determining the deformed fluid surface with a pinned contact line on a planar wall reduces to that of solving the pair of equations for the real functions $\tilde{y}(\sigma)$ and $\tilde{z}(\sigma)$:

$$\tilde{z}(\sigma) = h\Big(\sigma+\tilde{y}(\sigma)\Big) \qquad \text{and} \qquad \frac{\mathrm{d}\tilde{y}_+}{\mathrm{d}\sigma} + i\cos\theta_0\,\frac{\mathrm{d}\tilde{z}_+}{\mathrm{d}\sigma} = -\left(\frac{\mathrm{d}\tilde{y}_+}{\mathrm{d}\sigma}\right)^2 - \left(\frac{\mathrm{d}\tilde{z}_+}{\mathrm{d}\sigma}\right)^2\ . \tag{83}$$

We recall that $f_\pm$ are the projections onto positive (negative) momentum Fourier components of the function f. Continuing f_+ as an analytic function, F, in the upper-half $w=(\sigma+i\tau)/2$ plane, determines the unique harmonic extension of the function, $f = 2\,\mathrm{Re}F$. The conformally-parameterized minimal surface is

$$(x,y,z) = (\sin\theta_0\,\tau, \sigma+\tilde{y}, -\cos\theta_0\,\tau+\tilde{z}\,)\ , \tag{84}$$

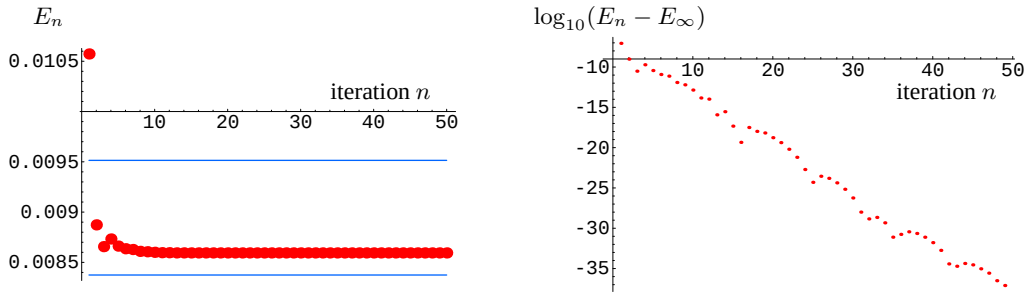

FIG. 3: Convergence of the energy E_n for a Gaussian with almost maximal amplitude, as function of iteration n. Also plotted are the perturbative results $E_2 = 0.00951444$, and $E_2 + E_4 = 0.00837429$. The second plot shows convergence on a $\log_{10}$ scale. Convergence improves considerably for smaller amplitude of h.

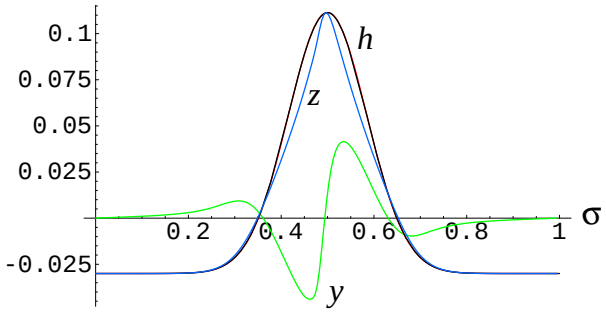

FIG. 4: A periodically repeated Gaussian for $h(y)$, with no 0-mode: $\int_0^1 \mathrm{d}y\, h(y) = 0$. The corresponding functions $y(\sigma)$ and $z(\sigma)$ on the boundary are also given. One remarks that z almost has a cusp-like singularity at $\sigma = 1/2$. Further increasing the amplitude of h, z will develop this cusp, which signals the breakdown of our parameterization.

and it has a total energy given by eqs. (40) or (41).

The equations (83) can be solved by iteration, starting with the initial configuration

$$\tilde{y}^{(0)}(\sigma) = 0 \ , \quad \tilde{z}^{(0)}(\sigma) = h(\sigma) \ . \tag{85}$$

Let $\tilde{y}^{(n)}$ and $\tilde{z}^{(n)}$ be the solution of the equations after n steps. We extract $\tilde{z}_+^{(n)}$ by doing a double Fourier transform. Plugging the result in eqs. (83) then gives the improved values of the unknown functions:

$$\tilde{y}_+^{(n+1)} = \int_{-\infty}^{\sigma} d\sigma' \left\{ \left[\frac{1}{4} - \left(\frac{d\tilde{z}_+^{(n)}}{d\sigma'} \right)^2 - i \cos\theta_0 \frac{d\tilde{z}_+^{(n)}}{d\sigma'} \right]^{1/2} - \frac{1}{2} \right\} \ , \quad \tilde{z}^{(n+1)} = h\left(\sigma + \tilde{y}^{(n+1)} \right) \ . \tag{86}$$

Using (41) yields an approximation E_n to the true energy E_∞. We have used this iterative algorithm for $h(y) = \varepsilon\, f(y)$ with $f(y)$ various trial pinning profiles. We found that it converges rapidly to the perturbative result for small ε, and that it breaks down at some critical ε where the function $y(\sigma)$ stops being monotonic. We believe this signals a coordinate, rather than a real geometric singularity, as is observed in section A. If so, it would be very interesting to develop alternative algorithms that could circumvent this problem.

On figure 3 we show the convergence of the algorithm at $\theta = \pi/2$ for a profile $h(y)$ given on figure 4, together with the corresponding functions $y(\tau)$ and $z(\tau)$. One sees on figure 4 already the emergence of a linear cusp at the tip of $z(\tau = 1/2)$, which signals for larger ϵ the break-down of the algorithm.

VIII. INTERACTION BETWEEN CONTACT LINES

As another application of the general approach, we will now calculate the interaction between the two contact lines of a liquid surface bounded by parallel walls. For an analogous calculation in open string theory see reference [25]. Suppose that wall 1 is

located at $x = 0$, wall 2 at $x = L$, and let $\gamma_1' = -\gamma_2' = \gamma\cos\theta_0$. In the absence of impurities the equilibrium configuration is thus an inclined planar surface making a contact angle θ_0 (respectively $\pi - \theta_0$) with the first (second) wall. We use conformal coordinates and set $x = \sin\theta_0\,\tau$, so that the parameter domain is the infinite strip $0 \le \tau \le L/\sin\theta_0 \equiv \tau_0$. Repeating the same steps as in the previous section leads to the following variational functional for the minimal area:

$$\tilde{\mathcal{A}}(\alpha_K, \tilde{y}, \tilde{z}) \;=\; \frac{1}{2}\iint_{0\le\tau\le\tau_0} (\partial_a\tilde{y}\,\partial^a\tilde{y} + \partial_a\tilde{z}\,\partial^a\tilde{z}) \;-\; \int_{\tau=0}\Big[\alpha_1\left(\tilde{z} - h_1(\sigma+\tilde{y})\right) \;-\; \cos\theta_0\,\tilde{z}\Big] \\ -\;\int_{\tau=\tau_0}\Big[\alpha_2\left(\tilde{z} - h_2(\sigma+\tilde{y})\right) \;+\; \cos\theta_0\,\tilde{z}\Big]\,. \tag{87}$$

Here $h_J(y)$ (for $J = 1, 2$) are the deformations of the two contact lines away from their equilibrium configuration, and α_J are the corresponding Lagrange-multiplier fields. The minimal area difference is $\tilde{\mathcal{A}}_{\rm min} \;=\; {\rm extr}\,\tilde{\mathcal{A}}$, where one must extremize $\tilde{\mathcal{A}}$ over the bulk fields $\tilde{y}(\sigma,\tau)$ and $\tilde{z}(\sigma,\tau)$ and the boundary fields $\alpha_J(\sigma)$.

First we solve the harmonic equations for $\tilde{y}$ and $\tilde{z}$, keeping their values on the boundary fixed. Let, for example, $\tilde{y}(\sigma,0) = \tilde{y}_1(\sigma)$ and $\tilde{y}(\sigma,\tau_0) = \tilde{y}_2(\sigma)$. Eliminating the field in the interior gives

$$\frac{1}{2}\iint_{0\le\tau\le\tau_0}\partial_a\tilde{y}\,\partial^a\tilde{y} \;\;\longrightarrow\;\; \frac{1}{4\pi}\sum_{J,J'}\int_\sigma\!\!\int_{\sigma'}\;\frac{{\rm d}\tilde{y}_J}{{\rm d}\sigma}\,G_{JJ'}(\sigma-\sigma')\,\frac{{\rm d}\tilde{y}_{J'}}{{\rm d}\sigma'}\,, \tag{88}$$

where

$$G_{JJ'}(\sigma-\sigma') \;=\; \begin{cases} -\log\sinh^2[\frac{\pi}{2\tau_0}(\sigma-\sigma')] & \text{if } \; J = J'\,, \\ -\log\cosh^2[\frac{\pi}{2\tau_0}(\sigma-\sigma')] & \text{if } \; J \ne J'\,. \end{cases} \tag{89}$$

One way of establishing this formula, is to start from the analogous expression for the unit disk, eq. (21), and then apply the conformal transformation that maps the unit disk onto the infinite strip:

$$v \equiv \sigma + i\tau = \;\frac{\tau_0}{\pi}\log\left(i\,\frac{1-w}{1+w}\right) \;\;\Longleftrightarrow\;\; w \equiv \rho e^{i\phi} = \tanh\left(\frac{i\pi}{4} - \frac{\pi v}{2\tau_0}\right)\,. \tag{90}$$

Notice that the two unit-radius semi-circles, $\rho = 1$ and $\phi \in [0,\pi]$ or $\phi \in [\pi, 2\pi]$, are indeed mapped onto the two boundaries of the strip, ${\rm Im}v = 0$ or ${\rm Im}v = \tau_0$. On these boundaries

$$\log\sin^2\left(\frac{\phi-\phi'}{2}\right) \;=\; \log\sinh^2\left[\frac{\pi}{2\tau_0}(v-v')\right] - \log\,\cosh\left(\frac{\pi v}{\tau_0}\right) - \log\,\cosh\left(\frac{\pi v'}{\tau_0}\right)\,, \tag{91}$$

up to an irrelevant constant. The terms depending only on v, or only on v', will drop out when inserted in the double integral (21). Setting finally $v - v' = \sigma - \sigma'$ (or $v - v' = \sigma - \sigma' - i\tau_0$) for points on the same (or opposite) boundaries of the infinite strip, leads to the expressions (88) and (89), as claimed. An alternative derivation of this result using the massless propagator on the strip is

$$G_{11}(\sigma) = \sum_{n=-\infty}^{\infty}\int\frac{{\rm d}k}{2\pi}\frac{{\rm e}^{ik\sigma}}{k^2 + (n\pi/\tau_0)^2} = \int\frac{{\rm d}k}{2\pi}\frac{{\rm e}^{ik\sigma}}{k^2} + 2\frac{\tau_0}{\pi}\sum_{n>0}\frac{1}{n}{\rm e}^{-n\pi|\sigma|/\tau_0} = -|\sigma| - \frac{2\tau_0}{\pi}\ln\left(1 - {\rm e}^{-\pi|\sigma|/\tau_0}\right) \tag{92}$$

$$G_{12}(\sigma) = \sum_{n=-\infty}^{\infty}\int\frac{{\rm d}k}{2\pi}\frac{(-1)^n{\rm e}^{ik\sigma}}{k^2 + (n\pi/\tau_0)^2} = \int\frac{{\rm d}k}{2\pi}\frac{{\rm e}^{ik\sigma}}{k^2} + 2\frac{\tau_0}{\pi}\sum_{n>0}\frac{(-1)^n}{n}{\rm e}^{-n\pi|\sigma|/\tau_0} = -|\sigma| - \frac{2\tau_0}{\pi}\ln\left(1 + {\rm e}^{-\pi|\sigma|/\tau_0}\right) \tag{93}$$

These formulae agree with (89) up to an irrelevant constant.

It will be useful to write these expressions in Fourier space. This can be done by using the identities

$$\sum_{n=-\infty}^{\infty}\frac{1}{b^2+n^2} = \frac{\pi}{b}\coth(\pi b)\,, \quad \text{and} \qquad \sum_{n=-\infty}^{\infty}\frac{(-1)^n}{b^2+n^2} = \frac{\pi}{b\sinh(\pi b)}\,. \tag{94}$$

To lighten the notation, we will suppress the label of the boundaries, and use boldface letters for the corresponding vectors and matrices. Thus $\tilde{\mathbf{y}}$ will stand for the two-component vector $(\tilde{y}_1, \tilde{y}_2)$, and $\mathbf{G}$ for the 2×2 matrix-valued kernel $G_{JJ'}$. With the help of the above formulae one finds:

$$\frac{1}{4\pi}\int_\sigma\!\!\int_{\sigma'}\;\frac{{\rm d}\tilde{\mathbf{y}}^{\,t}}{{\rm d}\sigma}\,\mathbf{G}(\sigma-\sigma')\,\frac{{\rm d}\tilde{\mathbf{y}}}{{\rm d}\sigma'} = \frac{1}{2}\int_k\tilde{\mathbf{y}}_k^{\,t}\,\widehat{\mathbf{G}}(k)\,\tilde{\mathbf{y}}_{-k} \quad , \tag{95}$$

where t indicates the transpose of a vector, and

$$\widehat{\mathbf{G}}(k) := k^2 \int_{-\infty}^{\infty} \mathrm{d}\sigma\, \mathrm{e}^{ik\sigma}\, \mathbf{G}(\sigma) = \begin{pmatrix} k\coth(\tau_0 k) & -k/\sinh(\tau_0 k) \\ -k/\sinh(\tau_0 k) & k\coth(\tau_0 k) \end{pmatrix} . \tag{96}$$

Since $\det \widehat{\mathbf{G}}(k) = k^2$, the inverse matrix takes also a simple form:

$$\widehat{\mathbf{G}}(k)^{-1} \;=\; \frac{1}{k} \begin{pmatrix} \coth(\tau_0 k) & 1/\sinh(\tau_0 k) \\ 1/\sinh(\tau_0 k) & \coth(\tau_0 k) \end{pmatrix} . \tag{97}$$

As a check note that in the limit of an infinitely-wide strip ($L \sim \tau_0 \to \infty$) one finds $\widehat{\mathbf{G}}(k) \simeq |k| \cdot \mathbf{1}_{2\times 2}$. This is indeed the kernel for two separate, half-infinite planes.

Returning to the variational functional (87), it can be replaced by

$$\tilde{\mathcal{A}}(\mathbf{a}, \tilde{\mathbf{y}}, \tilde{\mathbf{z}}) \;=\; \frac{1}{2} \int_k \left(\tilde{\mathbf{y}}_k{}^t \widehat{\mathbf{G}}(k)\, \tilde{\mathbf{y}}_{-k} + \tilde{\mathbf{z}}_k{}^t \widehat{\mathbf{G}}(k)\, \tilde{\mathbf{z}}_{-k} \right) + \int_k \left(\mathbf{a}_k \cdot \mathbf{H}_{-k} - \delta\mathbf{a}_k \cdot \tilde{\mathbf{z}}_{-k} \right) , \tag{98}$$

where $\mathbf{a} \equiv (\alpha_1, \alpha_2)$ is the vector of Lagrange-multiplier fields, $\delta\mathbf{a} \equiv \mathbf{a} - \langle \mathbf{a} \rangle = (\alpha_1 - \cos\theta_0, \alpha_2 + \cos\theta_0)$, and $\mathbf{H}_k$ is the Fourier transform of the (vector of) composite fields $h_J(\sigma + \tilde{y}_J(\sigma))$. Solving the linear equations for $\tilde{\mathbf{z}}$, and inserting the solution in the above functional gives

$$\tilde{\mathcal{A}}(\mathbf{a}, \tilde{\mathbf{y}}) \;=\; \frac{1}{2} \int_k \tilde{\mathbf{y}}_k\, \widehat{\mathbf{G}}(k)\, \tilde{\mathbf{y}}_{-k} - \frac{1}{2} \int_k \delta\mathbf{a}_k\, \widehat{\mathbf{G}}(k)^{-1} \delta\mathbf{a}_{-k} \;+ \int_k \mathbf{a}_k \cdot \mathbf{H}_{-k} \, . \tag{99}$$

We can now read off the Feynman rules that generalize the ones of the previous section. The propagators and 1-point functions for the vector fields are:

$$\begin{aligned} \text{——(} \quad &:= \; \langle\, \mathbf{a}_k \,\rangle \;=\; (\cos\theta_0, -\cos\theta_0)\, \delta(k) \\ \text{——} \quad &:= \; \langle \delta\mathbf{a}_k\, \delta\mathbf{a}^t_{-k} \rangle \;=\; \widehat{\mathbf{G}}(k) \\ \sim\!\sim\!\sim \quad &:= \; \left\langle \tilde{\mathbf{y}}_k\, \tilde{\mathbf{y}}^{\,t}_{-k} \right\rangle \;=\; -\widehat{\mathbf{G}}(k)^{-1} \, . \end{aligned} \tag{100}$$

The vertices do not mix fields on opposite boundaries, and are thus two copies of the vertices in (66).

Using these rules we may calculate the energy to any desired order in the h-expansion. The leading, quadratic energy that generalizes the JdG result reads:

$E_2^{\mathrm{strip}} = \gamma \Big($ 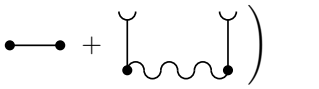 $\Big)$

$$= \gamma \sin^2\theta_0 \int_0^\infty \frac{\mathrm{d}k}{2\pi}\, k \left(\left(|h_{1,k}|^2 + |h_{2,k}|^2\right) \frac{\cosh(kL/\sin\theta_0) - 1}{\sinh(kL/\sin\theta_0)} \;+\; |h_{1,k} - h_{2,k}|^2 / \sinh(kL/\sin\theta_0) \right) . \tag{101}$$

Since both terms inside the integral are positive-definite, it is energetically favorable for $h_{1,k}$ and $h_{2,k}$ to have the same phase. Thus the interaction between the two contact lines is attractive. Note that if we fix h_1 and allow h_2 to freely adjust, we find that the minimum of the energy is obtained for

$$h_2(k) = \frac{h_1(k)}{\cosh(kL/\sin\theta_0)} \, . \tag{102}$$

The energy for given h_1 and free h_2 thus reads

$$E_2^{\mathrm{strip}}\Big|_{\text{free } h_2} = \gamma\, \sin^2\theta_0 \int_0^\infty \frac{\mathrm{d}k}{2\pi}\, k\, |h_{1,k}|^2\, \tanh\!\left(\frac{kL}{\sin\theta_0} \right) . \tag{103}$$

In the limit of $L \to \infty$, we recover our previous expression (52) as expected.

Taking the same limit in (101) shows that the interaction decays exponentially, as $\sim \exp(-2kL/\sin\theta_0)$. This exponential decay also applies for fixed L and very small contact angle, since the actual separation of the (unperturbed) contact lines is $L/\sin\theta_0$. In the opposite limit of a thin strip, or equivalently of very long-wavelength deformations, we find:

$$E_2^{\mathrm{strip}} \;\simeq\; \gamma \sin\theta_0 L \int_0^\infty \frac{\mathrm{d}k}{2\pi} \left[|h_{1,k} - h_{2,k}|^2 \left(\frac{\sin^2\theta_0}{L^2} - \frac{k^2}{6} \right) \;+\; \frac{k^2}{2} \left(|h_{1,k}|^2 + |h_{2,k}|^2 \right) \;+\; O(k^4) \right] . \tag{104}$$

The leading term has a simple geometric interpretation: It is proportional to the increase in area of a planar strip, whose boundaries undergo a relative displacement $h_1 - h_2$ along the walls, with which it made initially an angle θ_0. For $h_1 = h_2$, the next term in the above quadratic energy corresponds to an elastic rod with effective tension $\gamma_{\rm eff} = \gamma L \sin\theta_0$. This has also a simple geometric interpretation: The rod is in fact a thin strip, of width $L/\sin\theta_0$, which is deformed by an amount $h_1(y)\sin\theta_0$ in the transverse direction.

IX. DISCUSSION

In the previous sections we have shown how to calculate the energy of a deformed, almost rectilinear, contact line to any desired order in perturbation theory. We would now like to discuss some general properties of this expansion. One important point is that perturbation theory is *quasi-local*, i.e. the total energy is concentrated in a region of size equal to the typical wavelength of the deformation. We indeed saw that, as long as the large-volume cutoff has been fine-tuned so as to cancel the global tadpole, it decouples from any localized perturbation. One would expect the same to be true for all other geometric length scales of the system, such as the wall's inverse curvature. If this is true, at sufficiently short distances perturbation theory should be scale-covariant, as was pointed out in section V. In momentum space, the scaling symmetry (56) reads:

$$\tilde{E}[h^{(\lambda)}] \,=\, \lambda^2\, \tilde{E}[h] \qquad \text{for} \qquad h^{(\lambda)}_k = \lambda^2\, h_{\lambda k}\,. \tag{105}$$

Inspection of eqs. (68)–(82) shows that this indeed holds at each order of the expansion, and even for each individual diagram. Note, in passing, that the scaling symmetry does not imply conformal invariance, as would have been the case if the one-dimensional theory were truly local.

Finiteness of the JdG quadratic energy requires that

$$k h_k \to 0 \;, \quad \text{for both} \quad k\to\infty \;\; \text{and} \;\; k\to 0\,. \tag{106}$$

In other words, $h(y)$ must be continuous everywhere and finite, and it must vanish as $y\to\pm\infty$. A more stringent condition is, in fact, required to prove ultraviolet finiteness at all higher orders. It reads

$$k^2 h_k \to 0 \quad \text{for} \quad k\to\infty \quad \Longleftrightarrow \quad h^{(\lambda)}_k \to 0 \quad \text{for} \;\; \lambda\to\infty\,. \tag{107}$$

Stated differently, the profile function $h(y)$ must also have a continuous first derivative. That this is indeed necessary follows by considering for instance the "comb" diagrams, the first few being (78), (80) and (81). As the reader can check, a power fall-off slower than (107) would make the comb diagrams with a large enough number of vertices diverge. To show that this condition is also sufficient, it is convenient to assign the scaling dimensions $[k] = 1$ and $[h_k] = -2$ to the factors entering in a diagram. Because $k^2 h_k \to 0$ at high momentum, the degree of divergence of any partial integration is bounded from above by the corresponding scaling dimension, in which one only counts elements that depend on the integrated momenta. The scaling symmetry (105) implies that the overall scaling dimension of any tree diagram is -2, so there is no divergence from the integration region where all the momenta go to infinity. Keeping one (or more) of the momenta fixed amounts to removing from the counting a factor $\mathrm{d}k\, k^m\, h_k$, and at most one solid and m curly propagators that emanate from the corresponding vertex. This can only lower the scaling dimension, so all the partial integrations are also ultraviolet finite. *q.e.d.*

Infrared finiteness is trickier to establish diagrammatically. Condition (106) suffices to ensure that there is no divergence when the momenta flowing into individual vertices go to zero. The dangerous diagrams are, however, those for which such momenta *add up* to zero along some curly line. Inspection of the expression (54) shows, nevertheless, that the result is finite up to quartic order, thanks to the Heaviside functions that multiply such dangerous terms. To prove finiteness at all higher orders, it is more convenient to go back to the pair of classical equations (29) and (30). Let $\tilde{y}^{(n)}(\sigma)$ and $\tilde{z}^{(n)}(\sigma)$ be the solutions of these equations at nth order. It is then straightforward to check that, if these functions vanish at $y\to\pm\infty$ for all $n\le N$, they will continue to do so for $n = N+1$. This is in turn sufficient to guarantee the infrared finiteness of the energy at all orders.

What about non-perturbative effects? To fix ideas, let $h(y) = \varepsilon\, f(y)$ with $f(y)$ a given profile function, and ε the parameter controlling the perturbative expansion. One expects that the radius of convergence of this expansion is finite, since at large enough ε the solution to eqs. (29) and (30) should stop being analytic. This could signal either one of the following two things: (i) that our parameterization is singular, or (ii) that the surface develops real geometric singularities or that there is a change in topology. It would be very interesting to find some general criteria which could distinguish between these two possibilities. Note that a topological transition may occur if it is energetically favorable to drill two holes in the fluid surface, and to replace the corresponding disks by a cylinder. In any case, the following simple (though rather crude) linear bound

$$\tilde{E}[h] \,<\, \gamma \int_y |h| \,+\, \Big|\gamma' \int_y h\,\Big| \tag{108}$$

shows that the energy of a pinned contact line stays finite. Furthermore, localized microscopic perturbations always have a vanishingly-small energy, and should decouple from the physics at longer scales.

This brings us to our final remark [26]: as was explained in section II, the purely-Dirichlet minimal surface problem is related to the mixed Dirichlet-Neumann problem, relevant for capillary phenomena, by a Legendre transformation. A Legendre transformation looks at first sight rather benign, but it drastically modifies the nature of perturbation theory. This is best illustrated by the following spectacular phenomenon [27]: A wedge in the tubular contour $\partial\Omega$ of section II, with opening angle less than $|\pi - 2\theta_0|$, is a local geometric obstruction which forces the capillary surface to develop a second sheet. This has been observed in micro-gravity experiments. Notice that the wedge can be of microscopic transverse size, but it should extend to all values of the height coordinate z. It is the latter assumption which is responsible for the apparent non-decoupling of short-distance scales. The story is reminiscent of the role played by wormholes in theories of quantum gravity. This analogy, as well as the possible impact of wedge defects on the problem of wetting, deserve further investigation.

Acknowledgments: We thank Angelina Aessopos, Denis Bernard, François David, Matthias Gaberdiel, Gary Gibbons, Ramin Golestanian, Gian Michele Graf, Yves Pomeau, Elie Raphaël and Konstantin Zarembo for useful conversations. This research was partially supported by the European Networks MRTN-CT-2004-512194, MRTN-CT-2004-005104 and ANR program 05-BLAN-0099-01.

APPENDIX A: WEIERSTRASS PARAMETERIZATION

In section IV we have parameterized the minimal surfaces in terms of two functions $\tilde{Y}(w)$ and $\tilde{Z}(w)$, which are related by the conformal-gauge condition (30). The parameterization is global provided the two functions are analytic everywhere in the upper-half complex plane. This is indeed the case in perturbation theory, but more generally, for a given analytic $\tilde{Z}$, the solution of (30) will not give an analytic function $\tilde{Y}$. A constructive solution of the conformal-gauge condition, that guarantees analyticity, is given by the Weierstrass representation

$$\begin{pmatrix} X \\ Y \\ Z \end{pmatrix}(w) = \int_0^w \mathrm{d}v\, f \times \begin{pmatrix} 2g \\ -i(1+g^2) \\ 1-g^2 \end{pmatrix} \quad , \tag{A1}$$

where $f(v)$ and $g(v)$ are holomorphic functions in the upper-half plane. To go to the special gauge eq. (23) of section IV, one sets $2f = ic/g$. The surfaces are then parameterized by a single function:

$$\begin{pmatrix} X \\ Y \\ Z \end{pmatrix}(w) = \frac{ic}{2} \int_0^w \mathrm{d}v \begin{pmatrix} -2 \\ i(g+1/g) \\ g-1/g \end{pmatrix} \quad . \tag{A2}$$

Clearly, this special parameterization is non-singular if and only if g has no zeroes in the upper-half complex plane. Since in the expression (A1) both f and g are allowed to have any number of zeroes, this shows that the condition (23) need not always define a good global gauge.

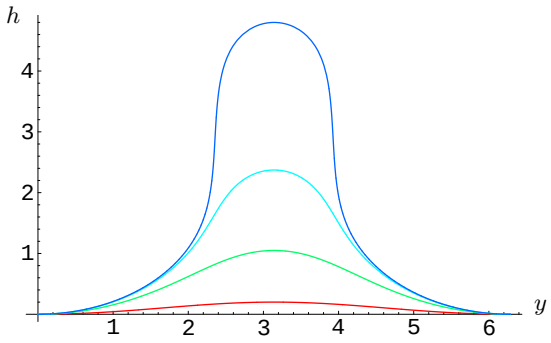

FIG. 5: Parametric plot of (A4) for $\kappa = 0.1, 0.5, 0.9, 0.999$. Increasing κ increases the amplitude of $h(y)$, and leads to a singularity at $\kappa = 1$. The function $\tilde{Z}(w)$ has been shifted s.t. $h(0) = 0$.

To describe the deformed surfaces of section IV we write

$$g = g_0 + \tilde{g}\ , \quad \text{with} \quad g_0 = \frac{\cos\theta_0 - 1}{\sin\theta_0}\ . \tag{A3}$$

The unperturbed planar surface corresponds to $\tilde{g} = 0$. Other choices of $\tilde{g}$, which are holomorphic in the upper-half plane (including the point at infinity) and for which $g_0 + \tilde{g}$ has no zeroes, describe globally-parameterized deformed fluid surfaces. As a simple example, let $\theta_0 = \pi/2$ and take

$$g(v) = -1 - \kappa\, \mathrm{e}^{2iv} \qquad \Longrightarrow \qquad \begin{aligned} \tilde{Y}(w) &= \frac{i}{4}\left[-\kappa \mathrm{e}^{2iw} + \log\left(1 + \kappa\, \mathrm{e}^{2iw}\right)\right] \\ \tilde{Z}(w) &= -\frac{1}{4}\left[\kappa\, \mathrm{e}^{2iw} + \log\left(1 + \kappa\, \mathrm{e}^{2iw}\right)\right] \end{aligned} \tag{A4}$$

where κ is a real parameter between 0 and 1, and in the expressions for $\tilde{Y}$ and $\tilde{Z}$ we have dropped an irrelevant constant [which can be absorbed in a redefinition of the origin of coordinates]. For small κ, this function describes a periodic minimal surface with period $\Delta y = 2\pi$, and with a deformed contact-line given by $h(y) = \kappa \cos y + O(\kappa^2)$. For κ finite, the contact-line profile is a complicated function given implicitly by eqs. (A4), and plotted on figure 5. Inserting the above $\tilde{Y}$ and $\tilde{Z}$ in the expression (40) for the energy gives:

$$\tilde{E}/\mathrm{period} = \frac{\pi\gamma}{4}\left[\kappa^2 - \log(1-\kappa^2)\right]\ . \tag{A5}$$

This reduces to the JdG energy at small κ, and can also be verified numerically. Note that when $\kappa \to 1$ the surface becomes singular, and the energy per period diverges.

APPENDIX B: MORE GENERAL LARGE-VOLUME CUTOFF

In this appendix we will repeat the calculation of the energy of section IV, using a more general container with an outer wall at an arbitrary inclination angle. The characteristic function $\Theta_C(\vec{r})$ now reads

$$\Theta_C(\vec{r}) \ = \ \Theta(x)\,\Theta\!\left(y + \frac{L_y}{2}\right)\Theta\!\left(\frac{L_y}{2} - y\right)\Theta(L_x - x\cos\phi + z\sin\phi)\ . \tag{B1}$$

The inclination angle ϕ of the outer wall is a control parameter, which should drop out in the $L_x, L_y \to \infty$ limit. The contact angle of the planar surface with this outer wall is equal to $\pi - \phi - \theta_0$, so Young's equilibrium condition requires that the corresponding solid-fluid tension be $\gamma'' = -\cos(\phi + \theta_0)$. Repeating the same steps as in section IV leads to the general expression for the energy

$$\tilde{E}[h] \ = \ -\frac{\gamma}{2}\oint_{\partial D} \Delta\vec{r}\cdot\partial_\perp\Delta\vec{r} \ - \gamma \oint_{\partial D} \Delta\vec{r}\cdot\partial_\perp\vec{r}_0 \ + \gamma \oint_{\partial\mathcal{D}} |\hat{n}\cdot\partial_\perp\vec{r}_0|^{-1}\,\hat{n}\cdot\Delta\vec{r} \ + \ \mathcal{E}_{\mathrm{bnry}}\ , \tag{B2}$$

where $\mathcal{D} = [0,\tau_0]\times[-L_y/2, L_y/2]$ is the parameter domain defined by $\Theta_C(\vec{r}_0) = 1$, $\partial_\perp$ is the derivative in the inward normal direction to $\partial\mathcal{D}$, and $\hat{n}$ is the three-dimensional vector normal to the container boundary.

We can now verify that the inclined wall does not contribute to the above expression. This follows from a fine cancellation between the three last terms in eq. (B2):

$$-\ \gamma\cos\theta_0 \int_\sigma \tilde{z} \ + \ \frac{\gamma\sin\phi}{\sin(\phi+\theta_0)}\int_\sigma \tilde{z} \ - \ \frac{\gamma''\sin\theta_0}{\sin(\phi+\theta_0)}\int_\sigma \tilde{z} \ \Bigg|_{\tau=\tau_0} \ = \ 0\ . \tag{B3}$$

We here used the normal vector $\hat{n} = (-\cos\phi, 0, \sin\phi)$, which implies that $|\hat{n}\cdot\partial_\perp\vec{r}_0| = \sin(\phi+\theta_0)$, as well as some three-dimensional geometry which is required to extract the contribution of $\mathcal{E}_{\mathrm{bnry}}$. Doing some straightforward trigonometry, and using the fact that $\gamma'' = \cos(\phi+\theta_0)$, one can check that the three terms (B3) indeed cancel. This confirms the decoupling of the large-volume cutoff, as was announced in section IV.

---

[1] See for instance J.C.C. Nitsche, *Introduction to minimal surfaces*, Cambridge U. Press (Cambridge 1989); U. Dierkes, S. Hildebrandt, A. Küster and O. Wohlrab, *Minimal surfaces*, vols. I and II , Springer-Verlag (Berlin 1991); R. Osserman, editor, *Minimal surfaces*, Springer-Verlag (Berlin 1997), and references therein.

[2] J.A.F. Plateau, *Statique expérimentale et théorique des liquides soumis aux seules forces moléculaires*, Clemm (Paris 1873).

[3] C. Isenberg, *The science of soap films and soap bubbles*, Dover (New York 1992).

[4] see e.g. A. Boudaoud, P. Patricio and M. Ben Amar, *The helicoid versus the catenoid: Geometrically induced bifurcations*, Phys. Rev. Lett. **83**, 3836 (1999) and references therein.

[5] D. J. Gross and P. F. Mende, *The high-energy behavior of string scattering amplitudes*, Phys. Lett. B **197**, 129 (1987);
C. Bachas and B. Pioline, *High-energy scattering on distant branes*, JHEP **9912**, 004 (1999) [arXiv:hep-th/9909171].

[6] P.G. de Gennes, *Wetting: statics and dynamics*, Rev. Mod. Phys. **57**, 827 (1985);
P.G. de Gennes, F. Brochard-Wyart and D. Queré, *Capillarity and wetting phenomena: drops, bubbles, pearls and waves*, Springer (New York 2004).

[7] T. Young, *An essay on the cohesion of fluids*, Phil. Trans. Roy. Soc. London **95**, 65-87 (1805).

[8] P.-S. Laplace, *Traité de mécanique céleste*, Courcier (Paris 1805).

[9] F. Hélein, *Constant mean curvature surfaces, harmonic maps and integrable systems*, Birkhäuser (Basel 2000).

[10] J.F. Joanny and P.G. de Gennes, *A model for contact-angle hysteresis*, J. Chem. Phys. **81**, 552 (1984); see also
Y. Pomeau and J. Vannimenus, *Contact angle on heterogeneous surfaces: weak heterogeneities*, Journal of Colloid and Interface Science **104**, 477 (1985).

[11] see for instance K. Sekimoto, R. Oguma and K. Kawasaki, *Morphological stability analysis of partial wetting*, Ann. Phys. **176**, 359 (1987), and references therein.

[12] R. Golestanian and E. Raphaël, *Relaxation of a moving contact line and the Landau-Levich effect*, Europhys. Lett. **55**, 228 (2001) [arXiv:cond-mat/0006496]; erratum, Europhys. Lett. **57**, 304 (2002); R. Golestanian and E. Raphaël, *Roughening transition in a moving contact line*, Phys. Rev. E **67**, 031603 (2003) [arXiv:cond-mat/0204531].

[13] P. Le Doussal, K.J. Wiese, E. Raphaël and R. Golestanian, *Can non-linear elasticity explain contact-line roughness at depinning?*, Phys. Rev. Lett. **96**, 015702 (2006) [arXiv:cond-mat/0411652] and to be published.

[14] A. Prevost, E. Rolley and C. Guthmann, *Dynamics of a helium-4 meniscus on a strongly disordered cesium substrate*, Phys. Rev. B **65**, 064517 (2002); S. Moulinet, C. Guthmann and E. Rolley, *Roughness and dynamics of a contact line of a viscous fluid on a disordered substrate*, Eur. Phys. J. E **8**, 437 (2002).

[15] P. Le Doussal, K.J. Wiese and P. Chauve, *2-loop functional renormalization group analysis of the depinning transition*, Phys. Rev. B **66**, 174201 (2002) [arXiv:cond-mat/0205108].

[16] A. Rosso and W. Krauth, *Roughness at the depinning threshold for a long-range elastic string*, Phys. Rev. E **65**, 025101 (2002).

[17] S. Moulinet, A. Rosso, W. Krauth and E. Rolley, *Width distribution of contact lines on a disordered substrate*, Phys. Rev. E **69**, 035103 (2004) [arXiv:cond-mat/0310173].

[18] see e.g. M. Ben Amar, L.J. Cummings and Y. Pomeau, *Transition of a moving contact line from smooth to angular*, Physics of Fluids **15**, 2949 (2003) and references therein.

[19] E. Giusti, *Minimal Surfaces and Functions of Bounded Variation*, Birkhäuser-Verlag (Basel 1984); R. Finn, *Equilibrium Capillary Surfaces*, Springer-Verlag (new York 1986).

[20] A. O. Caldeira and A. J. Leggett, *Influence Of Dissipation On Quantum Tunneling In Macroscopic Systems*, Phys. Rev. Lett. **46** (1981) 211; *Quantum Tunneling In A Dissipative System*, Annals Phys. **149** (1983) 374.

[21] C. G. . Callan and L. Thorlacius, *Open string theory as dissipative quantum mechanics*, Nucl. Phys. B **329**, 117 (1990).

[22] P. Le Doussal and R. Golestanian, unpublished.

[23] For a pedagogical reference see e.g. F. David, *Geometry and field theory of random surfaces and membranes*, in proceedings of the 5th Jerusalem school, D. Nelson et al editors, World Scientific (Singapore 1989).

[24] see e.g. R. Churchill, J. Brown and R. Verhey, *Complex Variables and Applications*, McGraw-Hill (New York 1975).

[25] C. Bachas, *Relativistic string in a pulse*, Annals Phys. **305**, 286 (2003) [arXiv:hep-th/0212217]; C. P. Bachas and M. R. Gaberdiel, *World-sheet duality for D-branes with travelling waves*, JHEP **0403**, 015 (2004) [arXiv:hep-th/0310017].

[26] C. Bachas, talk at Michael Green's 60th birthday, http://www.damtp.cam.ac.uk/eurostrings06.

[27] R. Finn, *Capillary Surface Interfaces*, Notices of the AMS vol. **46**, no. 7, and references therein.

[28] For calculational convenience the choice of convention here - see the propagators in e.g. Eq. (65) - corresponds to a weight $\exp(\tilde{\mathcal{A}}(\alpha,\vec{r}))$. This choice is immaterial since we are doing only a tree level calculation. One can equally well use the more physical choice $\exp(-\tilde{\mathcal{A}}(\alpha,\vec{r}))$ with $\alpha \to i\alpha$ and positive signs in all propagators, with identical final results at tree level.